RP-GSTAR-2021-001 DISSM/CGCT/INPE

STOCH2F: Stochastic two-flux code for diagnosis and assessment of solar radiative fluxes in the atmosphere

Part 1: 0.20-0.80 μm interval in clean clear-sky atmosphere

Juan Carlos Ceballos

January 2021

Abstract. The main scope of STOCH2F code is to develop a tool for analyzing interaction of solar radiation with gases, aerosol and clouds in Earth-atmosphere system. It is applied to a multilayered atmosphere, using two-flux approximation for radiative transfer in each layer together with a stochastic scheme for diffuse flux transfer between atmospheric layers. STOCH scheme describes absorption in each layer and ground as well as planetary reflection (photon exit outside Earth atmosphere) in terms of probabilities of trapping in a (final) absorption state, after a random up-and-down walk which starts as diffuse photon at a given (arbitrary) state in Earth-atmosphere system. The general structure is strictly equivalent to a random walk with a set of absorbing states, obeying a first order Markov chain. This scheme allows a better insight on radiative interaction between atmospheric layers.

Part 1 describes the philosophy and structure of the stochastic model, showing applications to an atmosphere without aerosol or clouds, with pure air and ozone as components. It does not consider presence of water vapor (bands 0.72 and 0.8 μm), with weak absorption and not monochromatic treatment. Further chapters will develop STOCH2F model for 1) solar infrared interval including H_2O and CO_2 absorption in clear-sky conditions; and 2) interaction of solar radiation with aerosol and cloud.

Contents

1. Introduction: irradiances in plane multilayered atmosphere

Model atmospheres for studies of radiative transfer within interval λ:(0.2-0.8 μm) are, typically, composed by plane-parallel layers. Each atmospheric layer is a mixture of air (basically oxygen, nitrogen and ozone) and aerosol (dry particles and/or droplets)([1]). Radiative transfer properties for solar *monochromatic* radiation are dependent of three bulk parameters: optical depth τ, single scattering albedo ω and phase function P(**Ω'**,**Ω**) for deviation from an incident direction **Ω'** towards a scattered one **Ω** (scattering angle Θ). Solar radiation impinging on the top of the atmosphere (τ=0) is attenuated with progressive absorption and/or scattering by air molecules; radiance field at depth τ is composed by directional irradiance Φ(τ, $\mathbf{\Omega}_o$) and a *diffuse* radiance $L(\tau, \mathbf{\Omega})$, where $\mathbf{\Omega}_o$ indicates downward direction coming from Sun (with zenithal angle *Z*o). Attenuation of monochromatic Φ_λ follows Beer's law,

$$\Phi_\lambda(\tau, \Omega_o)= S_\lambda(\tau, \mu_o)= S_{o\lambda} \exp(-m_o \tau); \qquad (1.1)$$

$S_{o\lambda}$ is the spectral solar constant at the top of atmosphere (TOA), corrected by Sun-Earth distance, and μ_o= cos *Z*o = 1/m_o. The diffuse field follows the radiative transfer equation (hereafter RTE)

$$\mu\, \partial L_\lambda(\tau,\Omega)/\partial\tau = - L_\lambda + (\omega/4\pi) \int_{2\pi} L_\lambda(\tau,\Omega')\, P(\lambda; \Omega',\Omega)\, d\Omega' + (\omega/4\pi)\, P(\lambda; \Omega_o, \Omega)\, S_\lambda(\tau). \qquad (1.2)$$

Equation (1.2) describes the rate of change of diffuse radiance through the contribution of: 1) (negative) attenuation by Beer's Law; 2) transfer of diffuse radiance from all directions **Ω'** towards **Ω**; 3) transfer $\mathbf{\Omega}_o \rightarrow \mathbf{\Omega}$ by scattering of direct radiation to diffuse. Bulk parameters (τ, ω, P(λ; **Ω'**,**Ω**)) are vertically inhomogeneous, but model atmospheres use to be divided in *N* homogeneous layers. These parameters are also spectral, being dependent on wavelength. Eqs. (1.1) and (1.2) refer to spectral irradiances (in units W.m^{-2}.μm^{-1}) or radiances (in units W.m^{-2}.μm^{-1}.ster^{-1}), indicated by subscript λ. For the ease of writing such subscript will be ignored. For details of equations (1.1) and (1.2), see Liou (2002), section 3.4.

Question: Which is the central radiative variable usually (and actually) sought in meteorology and climatology? *Answer*: The major interest is devoted to seek the vertical profile of radiative balance, in order to assess contribution of gases, aerosol and clouds to cooling/heating rate of each layer with thickness Δ*z* and the impact on dynamical and thermodynamical atmospheric processes. Figure 1 and eq. (1.3) resume the radiative balance in an atmospheric layer. Note that *Ea* (absorbed flux) is the quantity actually implied in radiative heating/cooling.

$$E_N(z)= E{\downarrow}(z) - E{\uparrow}(z),$$

$$\Delta E_N = -Ea = -\rho\, c_p\, \Delta z\, \partial T/\partial t = -(\Delta p/\gamma)\, \partial T/\partial t \qquad (1.3)$$

E_N	net irradiance (W.m-2)
ρ	air density (kg.m^{-3})
c_p	specific heat (J/kg °K)
γ	adiabatic lapse rate (°C m^{-1})
Δ*z*	layer thickness (m)
T	temperature (°K)
t	time (s)

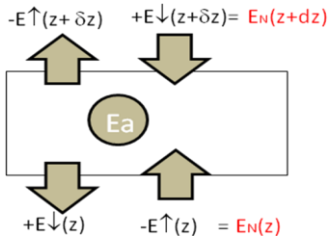

Figure 1. Flux components in radiative balance of a layer

[1] Weak absorption by water vapor (bands 0.72 and 0.8 μm) is not considered. A further chapter will analyze STOCH2F model for infrared interval including H_2O and CO_2 absorption.

Net irradiance $E_N(z)$ (or the term *Ea* in a layer) are important variables in weather and climate forecast by numerical circulation models (NMC's). Note that *irradiances* $E\downarrow\uparrow(\tau)$ rather than *radiances* $L(\tau, \mathbf{\Omega})$ are needed in eq.(1.3). Therefore, robust evaluation of two-flux methods are the goal of these applications. We denote by two-flux method a model for assessing upwelling and downwelling fluxes, or strictly speaking, irradiances.

Physical transfer properties of a layer can be assessed by complex codes (which are able to describe distribution of radiances emerging from the layer) or by simplified yet powerful algorithms assessing irradiances (Liou, 2002)([2]). All algorithms use the triad (τ, ω, $P(\Theta)$) as fundamental parameters in solutions of RTE (eq. 1.2), which can be reduced to a two-flux couple of equations for each layer (Zdunkowski *et al*. 2007; Liou 2002; Ceballos 1988):

$$dE\downarrow/d\tau' = -a_1 E\downarrow + a_2 E\uparrow + a_5 \omega \Phi \qquad (1.4)$$
$$dE\uparrow/d\tau' = -a_3 E\downarrow + a_4 E\uparrow + a_6 \omega \Phi.$$

Equation (4) describes evolution of diffuse irradiances $E\uparrow\downarrow(\tau')$ inside an homogeneous layer with optical thickness τ and constant parameters ω, $P(\Theta)$; Φ is solar directional flux. Coefficients a_1-a_6 depend on the adopted two-flux model ([3]). The general solutions for eq. (1.4) are not complex and allow calculation of irradiances $E\downarrow(0)$, $E\uparrow(0)$, $E\downarrow(\tau)$, $E\uparrow(\tau)$ for each layer, as well as the assessment of heating rate in eq. (1.3). However, assessing these irradiances requires to calculate four coefficients in compliance with layer's boundary conditions. This leads to a linear system of $4N$ unknowns which must be previously solved in order to assess irradiances and heating rate profile (Shettle and Weinman 1970).

The abovementioned methodology leads to provide final results for upward/downward irradiances in each layer and numerical solution for eq. (1.3); however, it does not contribute to get a deeper insight in how distribution of physical parameters influence on absorption profiles in the atmosphere. This paper presents a two-flux model which uses the same bulk properties of a multilayered atmosphere but introduces a stochastic point of view, providing simple tools for assessment of the entire absorption profile. It can also be used as a tool for better understanding the impact of photon generation at any level of that atmosphere.

2. **Looking at radiative transfer as stochastic process: basic concepts**

Let us consider *spectral* direct solar radiation impinging on the top with DNI (directional normal irradiance) Φ attenuates following exponential Beer's law being transmitted with DNI Φ_t; diffuse radiation has been generated, with resulting irradiances $E\uparrow$ emerging at layer's top and $E\downarrow$ exiting through layer's bottom. An irradiance E_a has been absorbed, and energy balance may be stated as follows (see figure 2a):

[2] In order to provide accurate results for RTE, two powerful softwares are worth of mention: SBDART (Ricchiazzi et al. 1998) and LibRadTran (www.libradtran.org/doku.php, newest release 2020; accessed 2021).

[3] Assessment of coefficients a1-a6 and solutions of two-flux equations are described in Appendix A.

$$\mu_o \Phi = E\uparrow_{top} + [E\downarrow_{bot} + \mu_o \Phi_t] + E_a, \quad (2.1)$$

$$\Phi_t = \Phi \exp(-m_o \tau), \qquad m_o = 1/\mu_o. \quad (2.2)$$

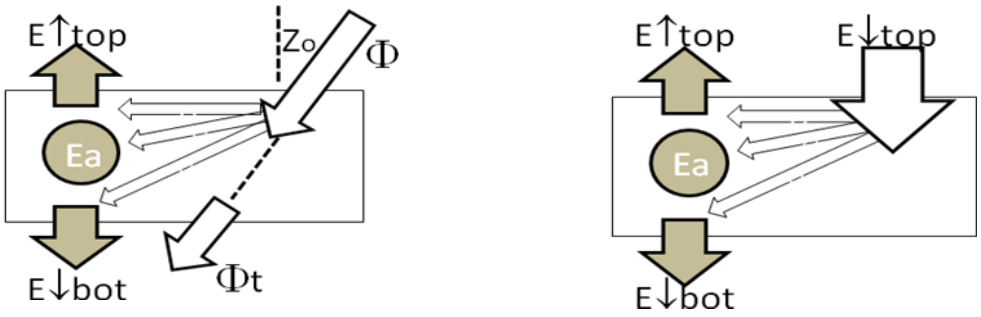

Figure 2. (a) Flux balance for direct solar radiation; (b) idem for diffuse incidence.

Irradiances Φ, E are spectral quantities. Zenithal angle for directional irradiance Φ is Z_o, with $\cos Z_o = \mu_o = 1/m_o$. The term within brackets is used to be called "global radiation", being the sum of a "direct" and a "diffuse" irradiance. Note that division of eqs. (2.1) and (2.2) by irradiance incident on top of the layer leads to a balance equation

$$1 = R_{oo} + T_{oo} + T_d + A_{oo}, \quad (2.3)$$

$$T_d = \exp(-m_o \tau). \quad (2.4)$$

Here, T_d is direct transmittance while R_{oo}, T_{oo} and A_{oo} are diffuse reflectance, diffuse transmittance and absorptance of the layer related to incidence of directional flux Φ with direction $\mathbf{\Omega}_o$. Note that incidence of a diffuse flux $E\downarrow_{top}$ leads to relations

$$E\downarrow_{top} = E\uparrow_{top} + E\downarrow_{bot} + E_a, \quad (2.5)$$

$$1 = R_o + T_o + A_o. \quad (2.6)$$

Reflectance R_o, transmittance T_o and absorptance A_o are related to layer properties for diffuse incidence (which <u>are not</u> the same as for direct incidence). Figure 2b illustrates the energy balance for diffuse fluxes.

Radiation fluxes may be interpreted in term of photons; for instance, N_λ (number/m^3.µm) being the spectral density of photons with wavelength λ flowing towards direction $\mathbf{\Omega}$, then directional flux Φ_λ [W.m^{-2}] in $\mathbf{\Omega}$ can be assessed by

$$\Phi_\lambda = N_\lambda \, c. \, h\nu. \quad (2.7)$$

Here, c is light speed and ν is photon frequency. Let us suppose that directional flux with zenith angle Z_o impinges on an horizontal surface: the flux per unit area (irradiance, in W.m^{-2}) through that surface will be

$$E_\lambda = \Phi_\lambda \cos Z_o = N_\lambda \, c. \, h\nu \, \mu_o \, . \quad (2.8)$$

Note that $E_\lambda / h\nu$ is the number of photons per unit time per unit surface crossing the surface.

Diffuse radiation exiting through the base of a plane layer is characterized by a distribution density $n(\mathbf{\Omega})$ in photons per unit volume per steradian (with $\mathbf{\Omega}$ indicating direction) so that associated physical fluxes in the base are

$n(\mathbf{\Omega})\, c\, h\nu = \delta F/\delta A_n.\delta\Omega$	flux of energy per unit area per steradian = <u>radiance</u> L [W.m^{-2}.ster^{-1}]. This is a directional variable!	(2.9)
$n(\mathbf{\Omega})\, c \cos Z\, h\nu = \delta F/\delta A.\delta\Omega$	$= L \cos Z$: flux of energy per unit area (direction Z) per steradian. Referred to direction normal to δA [W.m^{-2}.ster^{-1}]. This is refered to flux through	
$n(\mathbf{\Omega})\, c \cos Z\, h\nu .\, \delta A = I(\mathbf{\Omega})$	$= L \cos Z\, \delta A$: <u>intensity</u> (flux per steradian) emerging through δA [W.ster^{-1}] ([4])	
$\int_{2\pi} n(\mathbf{\Omega})\, c \cos Z\, h\nu .\, d\Omega = E\downarrow$	flux per unit area: <u>irradiance</u> [W.m^{-2}]	(2.10)

$N\downarrow_o = N_\lambda \cos Z_o\, c$	photons incident per unit area per unit time	
$\int_{2\pi} n(\mathbf{\Omega})\, c \cos Z\, d\Omega = N\downarrow$	photons exiting per unit area per unit time,	(2.11)

so that

$$E_\lambda\downarrow/\Phi_\lambda \cos Z_o = N\downarrow/N\downarrow_o = \text{Probability of diffuse transmittance} = P\downarrow((\tau, \omega, P(\Theta))\,|\,Z_o). \quad (2.12)$$

Eq. (2.12) describes probability of direct photons be transmitted as diffuse radiation (given the incidence with zenith angle Z_o); similarly, upward exiting photons would allow to define $P\uparrow = N\uparrow/N\downarrow_o$ as the probability of reflection for those incident photons. Note that for working with fluxes of photons per unit area, $\cos Z_o$ (incident) and $\cos Z$ (exiting) play a fundamental role in standardization of the number of photons.

The probabilities of diffuse transmission $P\downarrow_o$/reflexion $P\uparrow_o$ and also as de absorption Pa_o for direct incident photons will be identified with transmittance, reflectance and absorptance as solutions of the RTE (eq. 1.2) or the two-flux version (1.4):

$$P\downarrow((\tau, \omega, P(\Theta))\,|\,Z_o) = P\downarrow_o = T_{oo}. \quad (2.12$$

$$P\uparrow((\tau, \omega, P(\Theta))\,|\,Z_o) = P\uparrow_o = R_{oo}.$$

$$P_a((\tau, \omega, P(\Theta))\,|\,Z_o) = Pa_o = A_{oo}.$$

In the case of incident diffuse radiation, similarity of reasoning is obvious. Probabilities of transmission, reflexion, absorption of diffuse photons are paired with (T_o, R_o, A_o) obtained from RTE or two-flux image. Nevertheless, it must be noted that transfer properties of diffuse radiation should be influenced by the distribution density of incident photons; this can be seen, for instance, in diffuse reflectance

[4] These definitions were early built in the context of astronomy. The current term *radiance L* was *specific intensity,* that is, normally oriented intensity. French use is *luminance*.

$$P(\downarrow_{top} \rightarrow \uparrow_{top}) = \int_{-2\pi} n\uparrow(\mathbf{\Omega}) \cos Z\uparrow \, d\Omega \; / \; \int_{+2\pi} n\downarrow(\mathbf{\Omega}) \cos Z\downarrow \, d\Omega \; . \qquad (2.13)$$

Clearly, distribution $n\uparrow(\mathbf{\Omega})$ depends on the triad (τ, ω, $P(\Theta)$ but also on characteristics of downward incident radiation. A frequent hypothesis is that diffuse radiation is isotropic, that is, $n\downarrow$ and $n\uparrow$ are constant (not depending on $\mathbf{\Omega}$) but $n\downarrow \neq n\uparrow$.

Beer's law (eq. 1.1) can be interpreted as survival probability of photons within interval Δ: $[0,\tau)$:

$\Phi(\tau) = N(\tau) . c\, h\nu$,

$$\text{Prob}\{\text{no interaction in } \Delta\} = N(\tau)/No = \exp(- m_o \tau). \qquad (2.14)$$

Radiative transfer in a multilayered atmosphere can be thought of as a random walk of photons with frequency ν, in a complicated way:

- Vertical position is described in terms of optical depth, with photons travelling in straight lines with direction $\mathbf{\Omega}_1(Z_1,\varphi_1)$, Z_1= zenith angle and φ_1= azimuth.
- They interact randomly in optical paths $m\, \delta\tau$, $m = \cos Z_1$, according to exponential law (2.14).
- Then, they are scattered with probability

  $$\text{Prob}\{\text{scattering} \mid \text{interaction}\} = \omega, \qquad (2.15)$$

  $0 \leq \omega \leq 1$ (single scattering albedo), or absorbed with probability $1-\omega$.
- If scattered, they change direction $\mathbf{\Omega}_1 \rightarrow \mathbf{\Omega}_2$ according to a probability function given by a phase function $P(\Theta)$ which usually is axisymmetric:

  $$\text{Prob}\{\Theta' \subset [\Theta, \Theta+d\Theta)\} = P(\Theta)\, d\Theta. \qquad (2.16)$$
- But, $\mathbf{\Omega}_1$ and $\mathbf{\Omega}_2$ are vectors; so, Θ is a stochastic variable linked to phase function but describes a cone of possible scatterings defined by Θ and an azimuth ϕ which is also stochastic, defined by a constant probability density function:

  $$\text{Prob}\{\phi' \subset [\phi, \phi+d\phi)\} = d\phi/2\pi. \qquad (2.17)$$

Therefore, photons travel along a zig-zag of straight lines until a final situation or "state" of no return: absorption within atmosphere or at surface, or exit towards space (itself, another absorption state). Each line and scattering direction are defined by four basic probability numbers associated to eqs. (2.14-2.17). Successive extraction of random numbers defines "history' or "fate" of photons, allowing definition of probability distributions for final photon state. This is the principle of the so-called Monte Carlo method used for solving the RTE in complex 3-D structures, for instance cumuli populations (Barker and Davies 1992; Kargin and Prigarin 1994; Wen et al. 2008; Pincus and Evans 2009; Mayer 2009).

3. Multilayered atmosphere: Building a stochastic model

Consider a stratified atmosphere with N layers defined by triads $[\tau, \omega, P(\Theta)]_n$, n= 1, 2, ..., N as illustrated by figure 3. In such atmosphere, solar radiation impinges on the upper layer and is partially transmitted through the N layers, being absorbed and scattered in each one and establishing a field (actually a vertical profile) of upward and downward irradiances throughout the atmosphere. The fluxes through an interface between layers and those absorbed within a given layer are identified as *states* and numbered within a universe of $3N$+2 possibilities of existence of *diffuse radiation*. Note that states of absorption are numbered 1 (sky), 2 (ground), 3, ..., N+2. States of downward flux at interface between two layers are N+3, N+4, ..., (N+2)+N, while states of upward flux at interface between two layers are (2N+2)+1, (2N+4), ..., (2N+2)+N= 3N+2.

Directional flux Φo impinging the top of atmosphere will be progressively attenuated; for the n-th layer, this direct flux will generate diffuse or absorbed radiation as illustrated in figure 1(a). For instance, entrance at TOA will populate the fourth layer in figure 3 at states 6 (absorption), N+6 (diffuse transmission), 3N (diffuse reflexion) with fluxes (related to TOA)

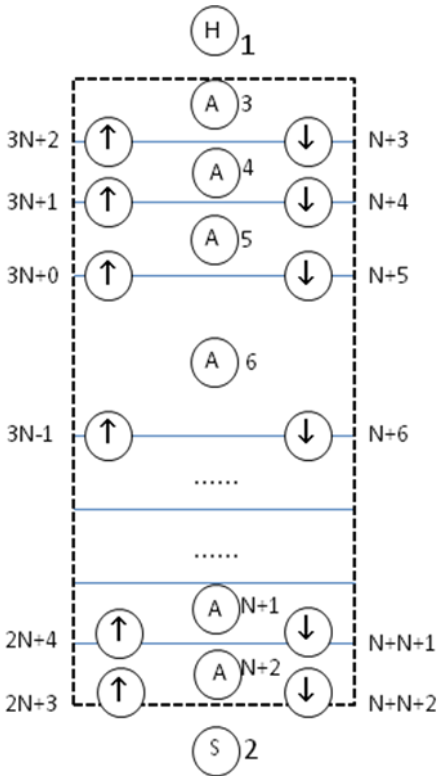

Figure 3. Transition states for diffuse radiation in a multilayered atmosphere.

$$P_o(6) = \exp(-m_o\,\tau 3)\,.\,A_{oo}(4), \qquad (3.1a)$$
$$P_o(N+6) = \exp(-m_o\,\tau 3)\,.\,T_{oo}(4),$$
$$P_o(3N+0) = \exp(-m_o\,\tau 3)\,.\,R_{oo}(4),$$

where $\tau 3=\tau_1+\tau_2+\tau_3$ is total optical depth of the three upper layers. P_o values can be thought of as *probabilities of initial diffuse states for direct radiation entering at TOA*. Further transfer of diffuse radiation can be seen as transition between states, the first possible jump representing *fractions of flux or transition probabilities*

$$Q(N+6\rightarrow 7) = A_o(5), \qquad (3.1b)$$
$$Q(N+6\rightarrow 3N\text{-}1) = R_o(5),$$
$$Q(N+6\rightarrow N+7) = T_o(5),$$
$$Q(3N\rightarrow 5) = A_o(3),$$
$$Q(3N\rightarrow 3N+1) = T_o(3),$$
$$Q(3N\rightarrow N+5) = R_o(3),$$

The set of probabilities $P_o(n)$, n=1,2,...,3N+2, defines a vector **P**o of first-state probabilities of diffuse radiation, and matrix **Q** with dimension (3N+2 × 3N+2) describes the set of probabilities of transition between states.

Two particular no-return states contribute to define global characteristics: state 1 (H for "Heaven") cumulates photons exiting the atmosphere; state 2 (S for "Soil") cumulates photons absorbed at the surface. Associated fist-state probabilities for them are

$$Po(1)= R_{oo}(1); \tag{3.2}$$

$$Po(2)= \exp(-m_o\, \tau N)\, .\, (1- Rs_{oo}). \tag{3.3}$$

Here, Rs_{oo} is ground reflectance for direct radiation. After this first situation, states will be progressively populated by diffuse transitions

$$Q(3N+2\rightarrow 1)= T_o(1), \tag{3.4}$$

$$Q(2N+2\rightarrow 2)=1-Rs_o, \tag{3.5}$$

Here, rs_o is surface reflectance for diffuse radiation. Reflectances Rs_{oo} and Rs_o for direct and diffuse radiation have identical values Rs for lambertian surfaces.

Clearly, if transition probabilities R_o, T_o, A_o for subsequent transfer jumps of diffuse flux are independent of the order of transition (this would be accomplished by isotropic diffuse radiance), then we have a definite triad $(R,T,A)_n$ for each one of N layers, and the entire sequence of transitions between states is a random walk described by a stationary first-order Markov chain, with transition matrix $\mathbf{Q}(3N+2 \times 3N+2)$ defined by $Q_{ij}= Q(\text{state } i \rightarrow \text{state } j)$. After k transitions, the probability vector for diffuse photon states makes

$$\mathbf{P}_k = \mathbf{P}_o\, \mathbf{Q}^k\, , \qquad \lim_{k\rightarrow\infty} \mathbf{P}_k = \boldsymbol{\pi} = \mathbf{P}_o\, \mathbf{Q}^{\infty}. \tag{3.6}$$

States n= 1, 2, ..., N+2 are absorbent, thus $Q\{n\rightarrow m\}= \delta_{n,m}$. Vector $\boldsymbol{\pi}$ describes probability of final states, being π_n=0 for n>N+2. The first N+2 (eventually non-null) components represent fractions of TOA direct irradiance $\mu_o\Phi$ which have been definitely allocated in the Earth-atmosphere system, being (a) reflected by the system (state H); (b) retained at soil (state S); or (c) absorbed within the atmosphere (states 3 to N+2). If this is the sought information, then eq. (13) does provide the solution of RTE in a multilayered atmosphere.

Estimation of $\mathbf{P}_o$ and $\mathbf{Q}$ allows for a straightforward procedure when comparing with the usual method needed in multilayered atmospheres. Following Shettle and Weinman (1970), this requires: 1) determination of general solutions for a two-flux method applied to each layer; 2) further application of inner and external boundary conditions ([5]), in order to evaluate upward and downward fluxes at each layer; 3) once defined boundary fluxes, assessment of energy balance for each layer.

The numbering of the set of states as shown in figure 2 allows to define the structure of $\mathbf{Q}$ and calculation of $\mathbf{Q}^{\infty}$ as (Cox and Miller 1965, Ceballos 1988)

$$\mathbf{Q} = \begin{vmatrix} \mathbf{I1} & \mathbf{O1} \\ \mathbf{U} & \mathbf{V} \end{vmatrix}, \quad \mathbf{Q}^{\infty} = \begin{vmatrix} \mathbf{I1} & \mathbf{O1} \\ \mathbf{W} & \mathbf{O2} \end{vmatrix}, \qquad . \tag{3.7}$$

[5] Internal conditions impose continuity at the boundaries of n-th layer: $E\downarrow(\tau'=\tau_n)_n= E\downarrow(\tau'=0)_{n+1}$, $E\uparrow(\tau'=0)_n= E\uparrow(\tau'=\tau_{n-1})_{n-1}$. For the upper layer it is $E\downarrow(\tau=0)_1= 0$, while for the lowest one we have $E\uparrow(\tau=\tau_n)_N = Rs_{oo} \exp(-\tau N/\mu_o) + Rs_o\, E\downarrow(\tau'=\tau_n)_N$, where $\tau N= \Sigma_n\, \tau_n$

$$\mathbf{W} = (\mathbf{I2} - \mathbf{V})^{-1}\,\mathbf{U}. \qquad (3.8)$$

Matrix dimensions are $\mathbf{Q}(3N+2 \times 3N+2)$, $\mathbf{I1}(N+2 \times N+2)$, $\mathbf{U}(2N \times N+2)$, $\mathbf{V}(2N \times 2N)$. Matrices $\mathbf{O1}(2N \times 2N)$ and $\mathbf{O2}(2N \times N+2)$ have null components. Matrix **I2** and **V** have same dimension.

As presented, the model allows to determine absorption profile for incoming direct radiation on TOA. Nonetheless, it is important to note that the initial vector $\mathbf{P}_o$ can be freely chosen. For instance, if the purpose is to seek the "fate of photons" produced by reflection on ground, it is enough to define $P_o(n)=0$ for all components but $P_o(2N+3)=1$. Vector π given by eqs. 13 and 14 yield the fraction of photons that will be absorbed in each layer.

Also, the fraction of diffuse radiation counter-reflected by atmosphere is R*, important for assessment of effects of successive reflections atmosphere-ground. In this case, we are interested in the transition $2N+3 \rightarrow 2N+2$. A single step would have probability $Q\{2N+3 \rightarrow 2N+2\} = Ro(N)$. But if all possibilities of transfer $\{2N+3 \rightarrow 2N+2\}$ within atmosphere are concerned, then the sought probability is found stating $Po(2N+3)=1$ and $Po(n \neq 2N+3)=0$, defining **Q** with $rs_o=0$, and calculating vector $\boldsymbol{\pi}$ (eq. 13); we assess $R^*=\pi(2)$, since any passage by transient state $2N+2$ implies in transfer to absorbing state 2.

Structure of matrix **Q** remained unchanged. This is an example of how the stochastic point of view defined by Figure 3 and eqs. (13) allows a deeper insight on radiative properties of a multilayered atmosphere. More details of the model can be found in Ceballos (1986, 1989) and Souza et al. (2008).

Comment on limiting matrix $\mathbf{Q}^{\infty}$

Due to zeros and low values of some coefficients in Markov matrix **Q**, some issues could be found in numerical inversion required by eq. (3.8). However, this low values (together with corresponding high values attributed to other transitions) suggest a steep convergence of $\mathbf{Q}^n$ to $\mathbf{Q}^{\infty}$. Therefore, adopted limit in eq. (3.7) may be, for instance, $\pi \approx P_{50}$. This is the solution adopted in present paper (included in subroutine function `Stoch2F.m`)

4. Physical parameters of a clean clear-sky atmosphere

The spectral range considered in this paper is Δ: 0.20-0.80 μm wavelengths. A clean clear-sky will be composed by air (oxygen O_2 + nitrogen N_2 in constant composition), ozone O_3, carbon dioxide CO_2 and water vapor H_2O. In a first approach, we consider

- absence of O_2 absorption lines at 0.63, 0.69 and 0.76 μm
- negligible influence of O_2 Herzberg continuum in 0.20-0.24 μm interval
- absence of weak absorption band of H_2O at 0.72 μm
- absence of background aerosol
- constant lambertian (isotropic) ground reflectance
- standard atmospheric profile of Mc Clatchey et al. (1972)
- solar spectrum of Gueymard (2004)
- Eddington approximation for radiative transfer (see Appendix A)
- An thirteen-layer atmosphere between z=0 and z= 70 km.

4.1. Atmospheric profile.

Two atmospheric profiles were considered: tropical (TROP) and Mid-Latitude Winter (MLW), following Mc Clatchey et al. (1972). From the original 64 levels, fourteen levels (thirteen layers) were extracted as shown in Table 1. Columns are: z (km): altitude, ro (g.m-3): density, p (hPa) pressure; O_3 (1E-5 g.m-3) ozone concentration. Layers are numbered from top to bottom: 1 (70-60 km), 2 (60-50 km), ... and so on. Mean concentration for ozone layers is assumed as arithmetic mean between altitudes.

Table 1. Atmospheric profiles (Tropical and Mid-Latitude Winter) following Mc Clatchey et al. (1972)

```
% ----- 13 layers McClatchey original
%  --- TROP -----     --- MLW ------
%z  ro     p   O3      ro    p     O3
70   .8  .058 .008     0.6  .047  .01; ...
60   .8   .40 .21      0.6  .300  .15; ...
50  1.1   .85  .43     0.89 .682  .43; ...
45  2.1  1.59 1.3      1.74 1.29  1.3; ...
40  4.2   3.0 04.1     3.62 2.53  4.1; ...
35 08.6   6.0 09.2     7.92 5.18  9.2; ...
30 18.3  12.2 24.0     17.8 11.1 19.0; ...
25 40.4  25.7 34.5       39 24.3 34.0; ...
20 95.1  56.5 19.0       87 53.7 45.0; ...
16  197   111   4.70     162  101 36.0; ...
10  420   286   3.90     407  257 16.0; ...
06  650   492   4.30     661  463  6.4; ...
03  876   715 5.10       923  694  4.9; ...
00 1167  1013 5.60      1030 1018  6.0];
% -------------------------------------
```

Figure 4 illustrates density profile of both atmospheres. It is seen that, except for the lowest layer and tropopause level (z~ 16 km), they are essentially the same. Figure 5 shows ozone profiles as given by McClatchey et al. (1972) and an expression fitted by Lacis and Hansen (1974, hereafter L&H) for O_3 integrated column (from ground to height z):

$$\nu(z) = \exp(z-b)/c, \qquad u_3(z)= a \,.\, (1 + \nu(0))/[1 + \nu(z)], \tag{4.1}$$

with a= 0.25 cm, b= 25 km, c=4 km (TROP) and a= 0.4 cm, b= 20 km, c= 5 km (MLW). Constant a (cm) refers to total O_3 column mass reduced to NTP condition (1013 hPa, 273ºK), so that 1 cm NTP = 21.43 g.m^{-2} ([6]).

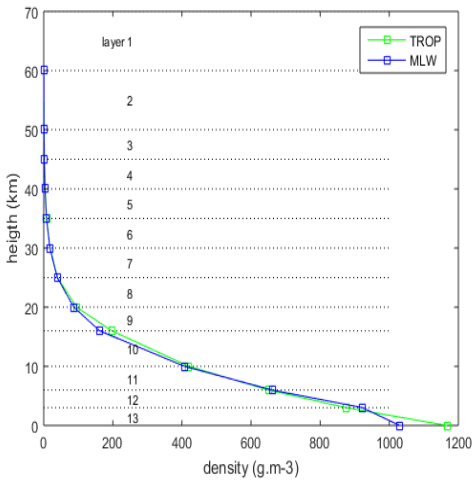

Figure 4. Density profiles for atmospheres TROP and MLW.

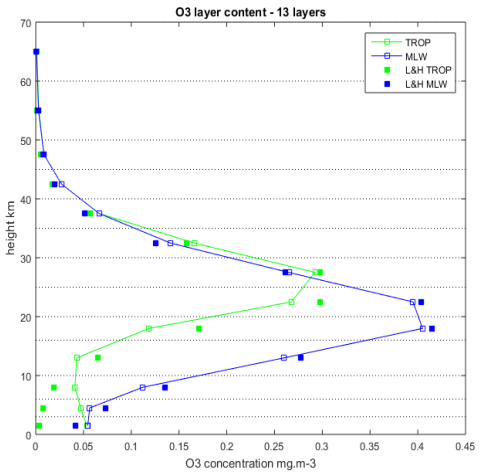

Figure 5. Ozone profiles for atmospheres TROP and MLW.

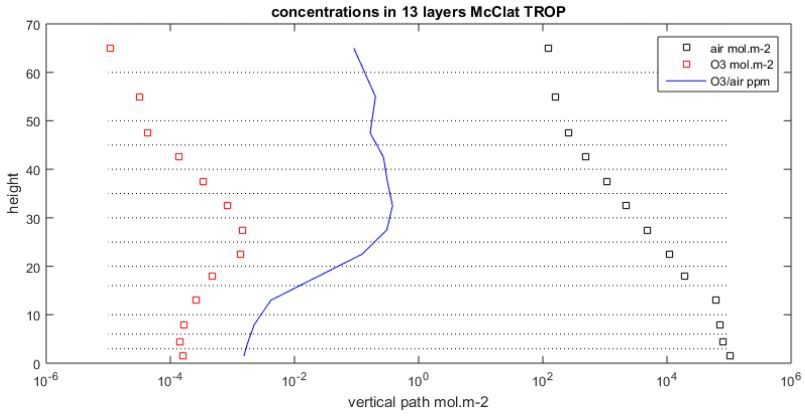

Figure 6. Air and O_3 contents in each one of 13 layers, in mol.m^{-2}. The blue line shows O_3 relative content , in parts per million.

[6] Ozone column is usually expressed in Dobson Units: 1000 DU = 1 cm O_3 in NTP conditions. Coefficients a= 250 DU , a= 400 DU fitted by L&H are coherent with profiles illustrated in Wallace and Hobbs (2006), Figure 5.16.

4.2. Solar spectrum.

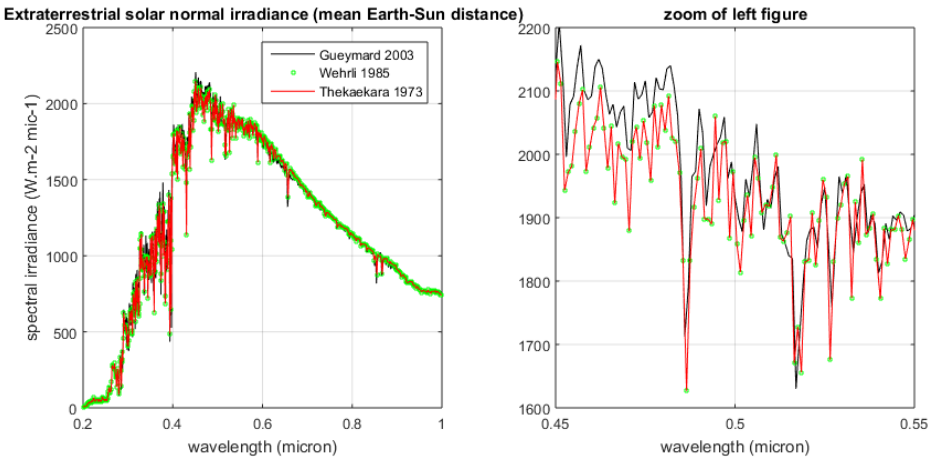

Figure 7. Solar spectrum (mean Earth-Sun distance) in 0.2-1.0 μm interval

Figure 7 shows three spectrums. Thekaekara (1973), Wehrli's 1985 NREL version and Gueymard (2004)([7]) seem equivalent; however, on the right hand the zoom makes evident equivalence of the first two while Gueymard's data show somewhat higher values (about 30-50 $W.m^{-2}.\mu m^{-2}$ at 0.45-0.48 μm, or about 2%). Spectral resolution of Gueymard spectrum is 1 nm= 0.001 μm; total irradiance S_o= 1366 $W.m^{-2}$. Integral values in our intervals of interest are

UV1	0.2-0.3 μm	15.5 $W.m^{-2}$	1.14 % of So (= 1366 $W.m^{-2}$)	
UV	0.2-0.4	111.2	8.14	
UVVIS	0.2-0.7	644.3	47.2	(4.2)
UVNIR	0.2-0.8	772.5	56.6	

4.3. Rayleigh scattering.

Spectral dependence of air Rayleigh scattering (ozone not included) for a column of p hPa is described by pure scattering (ω_R= 1) with asymmetry factor g= 0 and optical depth

$$\tau_R = 0.985^* 0.0088\ \lambda^{-4.15+0.2\lambda}\ (p/1013). \qquad (4.3)$$

This expression follows Paltridge and Platt (1976); factor 0.985 allows fitting to recent calculation by Bodhaine et al. (1999) within 1-2% in 0.3-1 μm interval.

[7] At NREL website https://www.nrel.gov/grid/solar-resource/spectra.html, the Wehrli, Thekaekara and Gueymad spectra are available as text files.

4.4. Ozone parameterizations.

Ozone molecular concentration is $N_3 = NA*[O3]/M_3$ (Avogadro's number NA= 6.02E23 molecules.mol^{-1}, molar mass M_3= 48 g.mol^{-1}). With concentration [O3] in g.m^{-3}, N_3 units are molecules.m^{-3}. The mean (homogeneous) value of N_3 at n-th layer was assumed as the arithmetic mean of two consecutive levels in Table 1. The corresponding optical depth is

$$\tau_3(n,\lambda) = N_3(n)\ \sigma_3(\lambda)\ dz(n). \qquad (4.4)$$

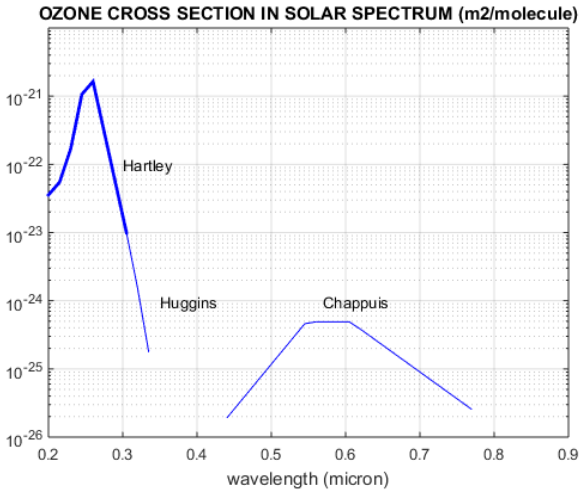

O_3 cross section (eq. 20) is described by Figure 5.

Optical depth τ_3 for a layer is assessed according to eq. (1) using

N_3 in molecules.m^{-3}

δz in km

σ_3 in m^2/molecule,

$$\tau_3 = N_3\ .\ 1E3\ \delta z\ .\ \sigma_3 \qquad (4.5)$$

Figure 5. Ozone cross section in solar spectrum

Molecular cross section σ_3 was interpolated from Liou (2002, figure 3.5) for three spectral bands: Hartley (0.20-0.315 μm), Huggins (0.315-0.35 μm) and Chappuis (0.45-0.79 μm), using the expression (coefficients in Table 2):

$$\log_{10}\sigma_3(\lambda) = c_2\lambda^2 + c_1\lambda + c_o, \quad (\sigma_3 \text{ in m}^2/\text{molecule}). \qquad (4.6)$$

Table 2. Ozone cross section parameterization (units σ_3 10^{-20} cm^2/molecule)

band	λ(μm)	c_2	c_1	c_o
Hartley	0.20-0.25	679.94	-269.8	4.314
	0.25-0.26	0	0	-20.73
	0.26-0.315	0	-49.25	-7.98
Huggins	0.315-0.34	0	-62.37	-3.86
(no band)	0.34-0.433			
Chappuis	0.433-0.55	0	13.18	-31.52
	0.55-0.61	0	0	-24.31
	0.61-0.782	0	-7.85	-19.55

4.5. Radiative properties of a layer

Fundamental parameters can be seen as stochastic events:

Probability of non-interaction in $(0,\tau) = \exp(-\tau)$, (4.7a)
Probability of interaction in $d\tau = 1- \exp(-d\tau) \approx d\tau$, (4.7b)
Probability of scattering | interaction$= \omega$, (4.7c)
Probability of scattering in $d\Theta$ | scattering $= P(\Theta)\ d\Theta$. (4.7d)

Given the homogeneous mixture of K components k=1,2, …, K, which are defined by triads $(\tau, \omega, P(\Theta))_k$,

$\tau = \Sigma_k \tau_k$, (4.8a)
Prob$\{k|$interaction$\} = \tau_k/\tau$, (4.8b)
Prob$\{$scatt$|$inter$\} = \omega = \Sigma_k (\tau_k/\tau)\ \omega_k$, (4.8c)

Probability of one photon interact in $d\tau$ <u>and</u> be scattered within $d\Theta$:

$d\tau\ .\ \omega\ .\ P(\Theta)\ d\Theta = \Sigma_k\ d\tau\ .\ (d\tau_k/d\tau)\ .\ \omega_k\ .\ P_k(\Theta)\ d\Theta$, therefore

$P(\Theta)\ d\Theta = \Sigma_k\ \tau_k\ \omega_k\ P_k(\Theta)\ d\Theta\ /\ \Sigma_k\ \tau_k\ \omega_k$. (4.8d)

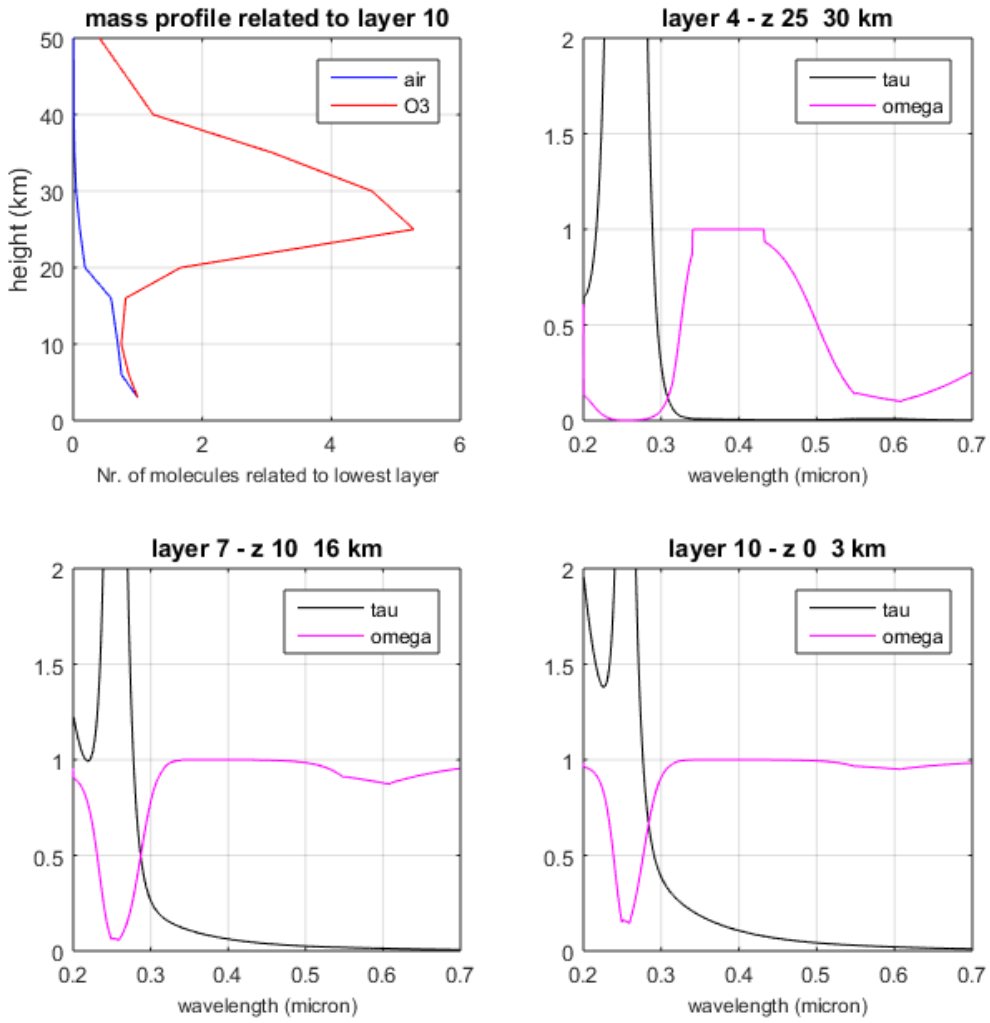

Figure 6. (a). Vertical profile of air and O_3 concentration (related to lowest layer), and (b-d) spectrums of total optical depth τ (eq. 4.7a) and single scattering albedo ω (eq. 4.7b) for three layers.

Within [0.25-1.0 μm] interval, air is not absorbent ($\omega_{air} = 1$) with Rayleigh scattering (optical depth τ_R), while ozone is purely absorbent ($\omega_3 = 0$) with optical depth τ_3. According to eqs. (20), a layer mixing air+O_3 will exhibit parameters

$$\tau = \tau_R + \tau_3, \qquad (4.9a)$$

$$\omega = \tau_R / (\tau_R + \tau_3), \qquad (4.9b)$$

$$P(\Theta) = P_R(\Theta). \qquad (4.9c)$$

Figure 6 illustrates some features of atmospheric profile. Subplot (a) shows rapid decrease of layers air mass, referred to lowest layer. Based on Table 1 data, it is represented the fraction $\Delta p(n)/\Delta p(10)$ for pressure of n-th layer. For O_3, it is used fraction $N_3(n)/N_3(10)$. It is seen that [O_3] is rather constant up to z=16 km; the peak concentration at 28 km is only 5 times the near ground value; however the relative optical depth is

$f = \tau_3/\tau_{air} = N_3 . \sigma_3/\tau_{air}$, (4.10)

so that $f>>1$ for Hartley band interval at all three layers, $f>1$ for Huggins band and $f<1$ for Chappuis band, and null within other intervals. This implies in $\tau>>1$ and $\omega\sim0$ for Hartley bands within stratosphere as seen in subplot (b), that is, total absorption of TOA solar irradiance in despite of $\omega>0$ in lower layers. Less intense than Hartley's, Huggins band is active in stratospheric levels, but weakly contributes to lowering ω in the troposphere. The same could be said about Chappuis band; however, larger influence on ω in the stratosphere should be compensated by the lower values of optical depth τ.

Concerning scattering, two-flux models use the *backscattered fraction* rather than function $P(\Theta)$. For energy coming from direction Ω_o, it is defined as the fraction b that is scattered into the original hemisphere (upward $\Omega\uparrow$, or downward $\Omega\downarrow$). Considering descending direction $\mathbf{\Omega}_o(\mu_o,\phi)$, ϕ = azimuthal angle, with phase function $P(\Theta)$, fraction b is

$$b(\mu_o) = b_o = \int_{2\pi\uparrow} 1/4\pi \, P(\Omega_o,\Omega\uparrow) \, d\mathbf{\Omega}\uparrow. \quad (4.11)$$

This is the backscattered fraction corresponding to direct radiation with zenithal angle Z_o (note it is independent of azimuth ϕ). For diffuse radiation with local radiance distribution $L(\Omega\downarrow)$, a mean backscatterd fraction is defined as

$$bmed\downarrow = \int_{2\pi\downarrow} b(\mu\downarrow) \, L(\mathbf{\Omega}\downarrow) \, d\Omega\downarrow \, / \int_{2\pi\downarrow} L(\mathbf{\Omega}\downarrow) \, d\Omega\downarrow. \quad (4.12)$$

A similar average $bmed\uparrow$ can be defined for backscattering of ascending diffuse radiation. In the case of a mixture O_2+air, phase function is the Rayleigh scattering function

$$P_R(\Theta) = 3/4 \, (1 + \cos^2 \Theta) = 1 + P_2(\mu^*)/2, \quad (4.13)$$

with $\mu^* = \cos(\Theta)$, P_2 = 2nd degree Legendre polinomial. For this phase function, any distribution $L(\mathbf{\Omega})$ yields

$$b_R(\mu) = bmed\uparrow\downarrow = 1/2. \quad (4.12)$$

Backscattered fractions are currently parameterized with respect to phase function assymetry factor

$$g = \int_{4\pi} P(\Theta) \cos(\Theta) \, d\mathbf{\Omega}. \quad (4.14)$$

For Rayleigh scattering, asymmetry is null: $g=0$.

As a matter of fact, the actual parameter triad in two-flux models is $\{\tau \; \omega \; g\}$. Transfer properties (R_{oo}, T_{oo}, A_{oo}) for direct and (R_o,T_o,A_o) for diffuse radiation in each layer are found solving the couple of eqs. (4), considering null reflectance at the bottom of the layer. Appendix A describes solution for the set of layers of Table 1.

4.6. Surface parameters

It was assumed lambertian reflection for all types of surface. Spectral characteristics were taken from JPL Laboratory files (Baldridge et al. 2009) and SBDART files based on Reeves et al. (1975). Figure 7 illustrates several spectrums for current surfaces.

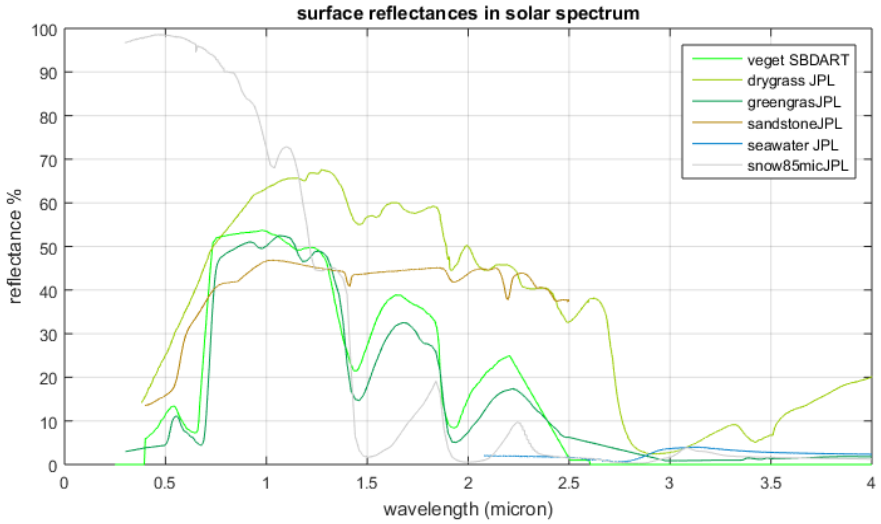

Figure 7. Ground reflectance for several surfaces

5. Applications to a clean clear-sky atmosphere

As commented in Section 3, adopted solution of eq. (13) was $\pi \approx P_{50}$. Rapid convergence of $\mathbf{Q}^k$ allowed this assumption. In the following, we present six examples of application of STOCH2F code and show how a stochastic-based reasoning can highlight understanding of solar radiation transfer in the atmosphere.

5.1. Absorption spectra in four layers, clear-sky conditions

Figures 7 show results of the spectrum of absorption probabilities of direct radiation impinging on the top of atmosphere, for Zo= 60º and Rs= 0.5. Four layers are illustrated: above peak of O_3 concentration (45-50 km), at the peak (25-30 km), upper troposphere/low stratosphere (10-16 km) and at the lower layer (0-3 km). Note that below the peak the probabilities scale is 10 ten times lower than above it. High Z_o and *Rs* values were chosen in order to enhance probabilities of scattering/absorption. Initial and final probabilities [P_o(layer) and $P_{final} = \pi$(layer)] are shown in green and black, respectively. We can see that:

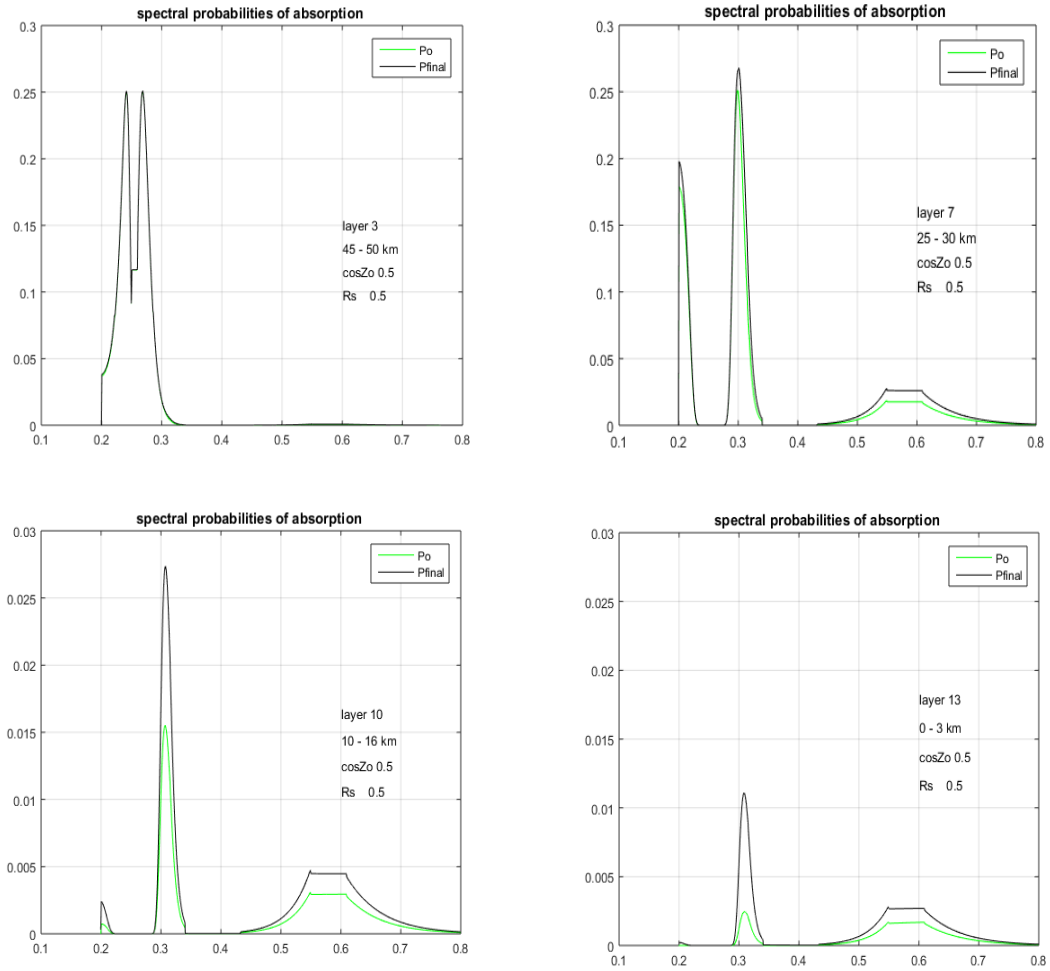

Figure 7. Spectrum of absorption probabilities in UVNIR interval (0.1-0.8 μm). Layers 3, 7, 10, 13. TROP atmosphere, incidence Z_o= 60º, ground reflectance *Rs*= 0.50. Green (black): initial (final) probabilities.

- Layer 3 (45-50 km): Hartley and Huggins bands are strongly present with absorption probabilities $\pi(5)$~0.25, while Chappuis band weakly appears. Green and black spectrums are identical, making evident that descendent photons no more return if passing through the stronger bands of this layer. Of course, upward photons can circulate across the layer (but outside stronger bands) as reflected radiation.
- Layer 7 (25-30 km), with highest O3 concentration: high absortance in Hartley and Huggins bands, as well as sensible absorption in Chappuis band. It is seen that photons upcoming from lower layers (with impact of high ground reflectance) contribute to total absorption (less than 20% of original absorption).
- Layer 10 (10-16 km): high absorption within upper layers has minimized contribution to Hartley band; Huggins is predominant (with 40% of additional contribution of upward photons absorption). Chappuis band is always weaker but shows significant contribution of upward flux absorption. Final probabilities $\pi(10)$ are ten times smaller than above tropopause. The spectrum in layer 13 (0-3 km) is similar to layer 10, but probabilities $\pi(13)$ are 2.5 times smaller.

It is concluded that strong absorption almost eliminates solar radiation at ground level for $\lambda < 0.3$ μm. Multiple reflection within atmosphere can collaborate to final absorption especially in lower layers and Chappuis band (because solar spectrum is higher in VIS than in UV interval). These results suggest that atmosphere below 16 km shows weak absorption of solar radiation, even in the presence of highly reflecting surfaces.

What should happen to upward radiation? How able is it of exiting into space (state 1)? The stochastic model yields some clear information about that. Figure 8 shows the fate of three kind of initial situations of the 13-layered atmosphere: 1) fate of a direct photon on TOA; 2) diffuse upward photons beginning at ground level (state 29); 3) diffuse upward photons passing through 16 km level (state 33), exiting layer 10. Direct beam at TOA has zenith angle $Z_o = 60^o$ ($\mu_o = 0.5$), TROP atmosphere.

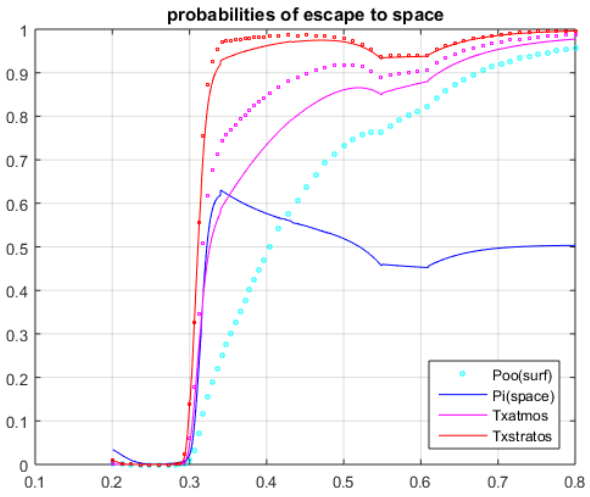

Figure 8. Probabilities of scape into space (as planetary reflectance). TROP atmosphere, Zo= 60º.

- Photons impinging at TOA: the line in blue describes the spectrum of exit through state 1, $\pi(1)$, and cyan dots describe the first impact (direct+diffuse) with Po(surf)= Po(2)/(1-Rs). Nearly all radiation in $\lambda<0.3$ μm is absent in both cases (since upper layers have very low backscattering, and descending photons have been absorbed by Hartley/Huggins bands). A steep increase of $\pi(2)$ is seen for $\lambda>0.3$ μm, due to lowering absorption by Huggins band and strong to backscattering by high Rayleigh optical mass; however, for $\lambda>0.32$ the decrease of scattering and the presence of Chappuis band can be seen. Increased transmittance of atmosphere (see cyan dots) and high soil reflectance also contribute to $\pi(1)$; for higher λ, it is seen the limiting situation of very high transmittance of downward and upward radiation. Thus, fraction Rs= 0.5 of inicial irradiance goes back to space.
- Diffuse photons starting at ground (state 29): the stochastic walk state 29 $\rightarrow$ state 1 has initial probability vector P_o with dimension 41, with null components except $P_o(29)= 1$, and final state probabilities $\pi \sim P_o \mathbf{Q}^{50}$. Figure 8 shows $\pi(1)$ in magenta, considering *Rs*=.5 (dots) and *Rs*=0 (line)([8]). It is seen that only photons with $\lambda>0.3$ are able to escape into space. The effects of Chappuis band can be seen; for high λ $\pi(1)\rightarrow 1$. The increase of $\pi(1)$ due to atmospheric backscattering and multiple reflections on ground is not negligible (0.73 to 0.85 at $\lambda=0.4$; 0.85 to 0.89 at $\lambda=0.55$**,** region of solar spectrum maximum). The spectrum is similar to blue line, except that this one includes the weighting with probability of attenuation before getting surface.
- Starting at stratosphere (state 33, at z=16 km), ascending photons are strongly absorbed by Hartley band but only partially by Huggins. In the presence of *Rs*=0.5 (red dots) and $\lambda>0.32$ μm, $\pi(1)\sim0.98$ but Chappuis band can reduce the exit to level $\pi(1)= 0.94$. For simulating the effect of stratosphere only, absorbing condition was attributed to state 24 (descending radiation at 16 km). So, for transition matrix Q(i,j) we stated null reflection and absorption and unit transmittance in layers 10-14, together with *Rs*=0. Therefore, incidence on state 24 yields direct transition to state 2 and only stratospheric stochastic walk is performed. It is seen that although transition $29\rightarrow1$ has a high probability $\pi(1)$, it is about 0.95 in the maximum of solar spectrum and even presents the effect of Chappuis band ($\pi(1)\sim0.93$). Concerning satellite observations (usually in $\lambda\sim0.6$ and $\lambda\sim0.8$), reduction of information $\pi(1)$ to original Po(29) would require a slight correction in VIS channel and none in NIR channel, except for anisotropy of exiting radiation:

$$\pi(1)\ \mu_o\ S_\lambda = E_\lambda \text{ (measured)} = P_o(29)\ \ \mu_o\ S_\lambda\ .f\ T_\lambda \qquad (5.1)$$

Concluding: Hartley band acts as a photon trap. Neither photons incident at TOA arrive to ground, nor upward photons from ground or tropopause levels attain the outer space. The same partially happens with Huggins band, although some transmission is allowed at $\lambda>0.3$ μm.

5.2. Vertical profiles of absorption in clear-sky conditions

Figures 9 show the profile of energy absorption obtained for different solar zenith angles. Only ozone is responsible for absorption. The absorbed irradiances ΔE are probabilities π weighted with solar spectrum S_λ at top of atmosphere (hereafter TOA):

[8] The direct influence of *Rs* appears in two terms of transition matrix: Q(28,2)= 1-Rs, Q(28,29)= Rs.

$$\Delta E(\text{layer}, \mu_o) = \sum_i \pi(\lambda_i, \text{layer}, \mu_o).\ \mu_o\ S_\lambda(\lambda_i)\ \delta\lambda_i \qquad (5.2)$$

$$F(\text{layer}, \mu_o) = \Delta E/\Delta z; \qquad (5.3)$$

F is the profile or absorption rate in W.m^{-2}/km in the layer with geometric thickness Δz.

Figures show profiles for interval UV(0.2-0.4 m), UVVIS (0.2-0.7 m) and UVNIR (0.2-0.8 μm) and include the final flux F (continuous lines) as well as the contribution of initial probability vector P_o (dotted lines), say $F_o(z)$. High value of ground reflectance (Rs=0.5) enhances the effect of further scattering. It is seen that for vertical incidence absorption rate at layers 7-8 (maximal O_3 concentration, figure 5) increases by about 50% (from 1.1 to 1.7 W.m^{-2}.km^{-1}) in UVVIS as well as UVNIR spectral ranges. For slant incidence (Z_o≥75°), absorptance is higher but TOA irradiance is lower, leading to lower F_o and F profiles; also, higher absorption before arriving at surface (lower $P_o(2)$) leads to lower relative contribution of multiple scattering.

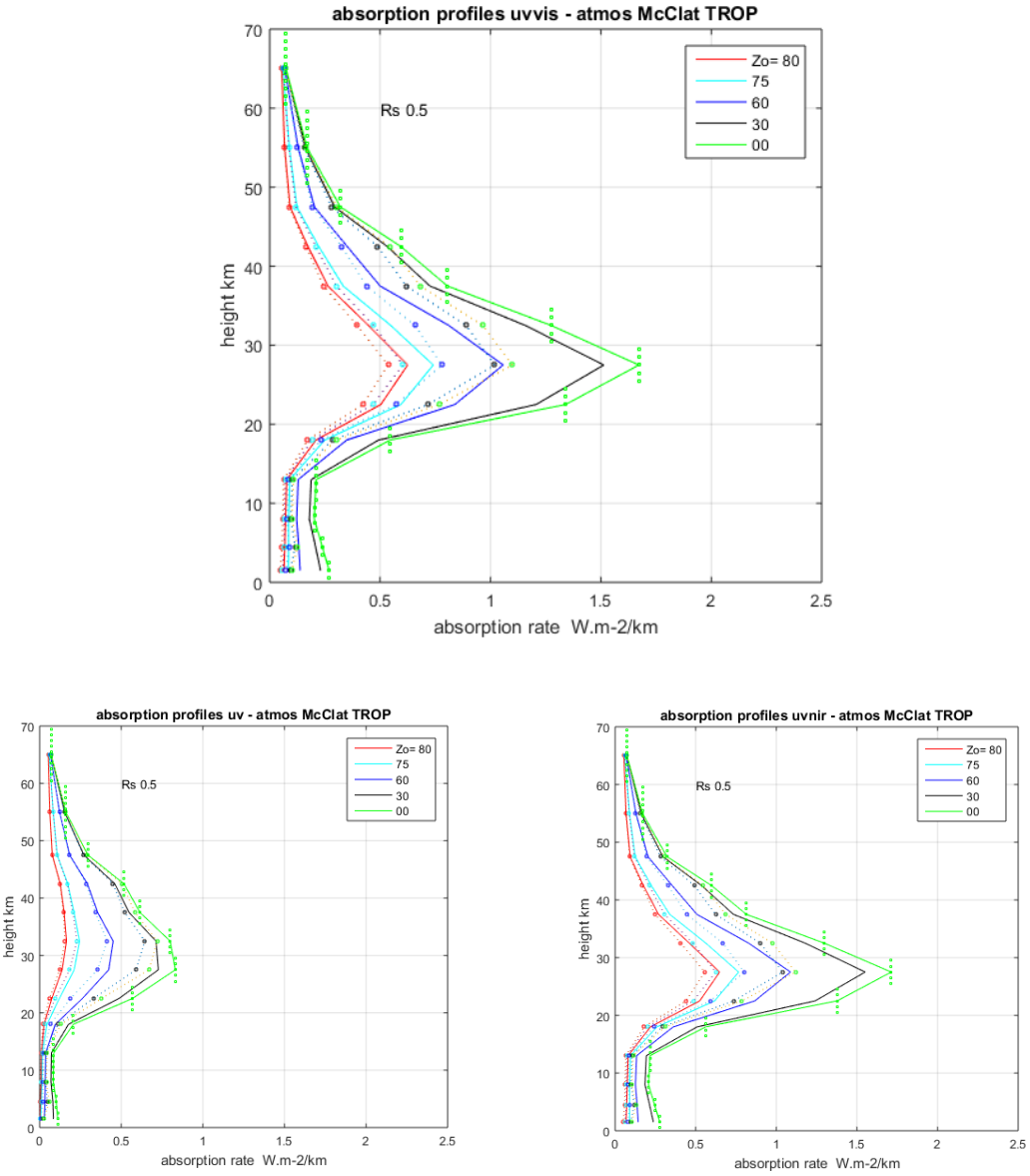

Figures 9. Absorption profiles in three spectral intervals: UVVIS, UV and UVNIR

Comparing UV and UVNIR diagrams, it is seen that the highest UV value is about 50% or less than total absorption, showing that higher absorptance of Hartley/Huggins in UV is compensated by higher TOA irradiances in the weaker Chappuis band interval.

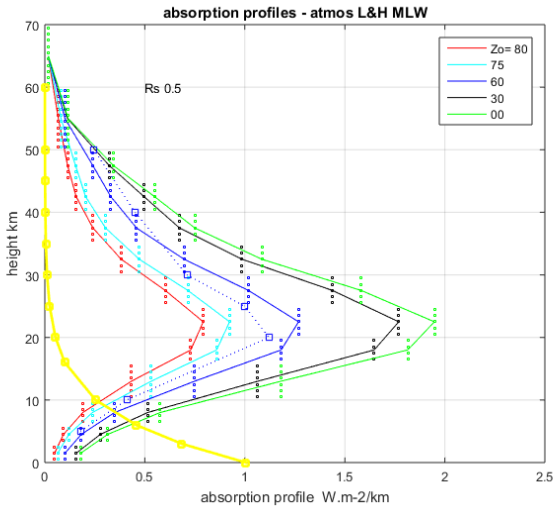

Figure 10. Absorption profiles in MLW atmosphere.

Figure 10 shows absorption profiles in MLW atmosphere. Maximal absorption is at lower height than TROP case. Blue squares illustrate profile reported by Lacis & Hansen (1974) for Z_o= 60º. They used O_3 profile given by eq. (4.1) and US standard atmosphere, applying a high quality radiative transfer code (doubling-adding). It is seen that the STOCH2F algorithm exceeds LH's by about 0.1-0.2 $W.m^{-2}.km^{-1}$ but depicts the same profile.

The figure includes the pressure fraction $p(z)/p(z=0)$, in yellow. Concerning heating rates, it can be expected to be very low at the troposphere (z<10 km), and the maximum be displaced to higher altitude, due to decreasing pressure (thus, density of enthalpy absorber layers).

Figures 9 make evident that, in spectral interval 0.2-0.8 μm, atmosphere can be divided in two regions. First, a tropospheric region (z≤16 km) where O_3 absorption is low in clear-sky conditions (less than 0.25 $W.m^{-2}.km^{-1}$, or about 4 $W.m^{-2}$) and would be even lower in the presence of cloud and aerosol. This region contains the current meteorological phenomena and their thermodynamic and dynamic energetic balance.

Secondly, a stratospheric region (16 < z < 70 km) contains a radiative O_3 sink which is fed not so much by scattering but mainly by the feedback of solar radiation reflected by the lower layer and surface (the case of snow or sand would be particularly important). In any case, strong Hartley band leads to zero fluxes returning to space or attaining surface (see figure 8). Higgins band allows the presence of fluxes for λ> 0.3 μm. Chappuis band may assume not negligible rol in the surface-atmosphere-space radiative balance.

In what follows, we divide Earth-atmosphere system in four layers: outer space (z>60-70 km), stratosphere (16<z<60 km), troposphere (z≤ 16 km), ground.

5.3: Energy partition between ground, space and atmosphere

We assume troposphere as low absorption layer below 16 km (layers 10-13) and stratosphere as z>16 km (layers 1-9). Absorption probabilities in the stratosphere (states 3-11) and troposphere (states 12-15) will be

$$A(\text{strat})= \Sigma_{i=3,11}\ \pi(i), \qquad A(\text{trop})= \Sigma_{i=12,15}\ \pi(i). \tag{5.4}$$

Absorption probability into space π(1) corresponds to planetary reflectance *Rp*. Absorption into ground π(2) is related to irradiance *GL* (direct+diffuse) incident on Surface; in UVNIR interval,

$$\pi(2) = (1\text{-}Rs).\ GL/(\mu_o\ S_{uvnir}) \qquad (5.5)$$

Eq. (5.5) expresses the fact that the probability of absorption into ground $\pi(2)$ is the probability of photons strike ground, times the probability of not being reflected (1-*Rs*). Of course, this simple relationship over UVNIR interval is valid for constant *Rs* (independent of wavelength). Figures 11 show the four spectral probabilities as well as the spectral irradiances for Zo=60º, Rs=0.2. Solar TOA irradiance is also shown, as well as spectral bands of channels 1 and 2 of ABI GOES 16 sensor (Schmit et al. 2017). It is evident that observation with only one channel (usually number 2) would fail in describing complexity of exiting irradiance (blue line).

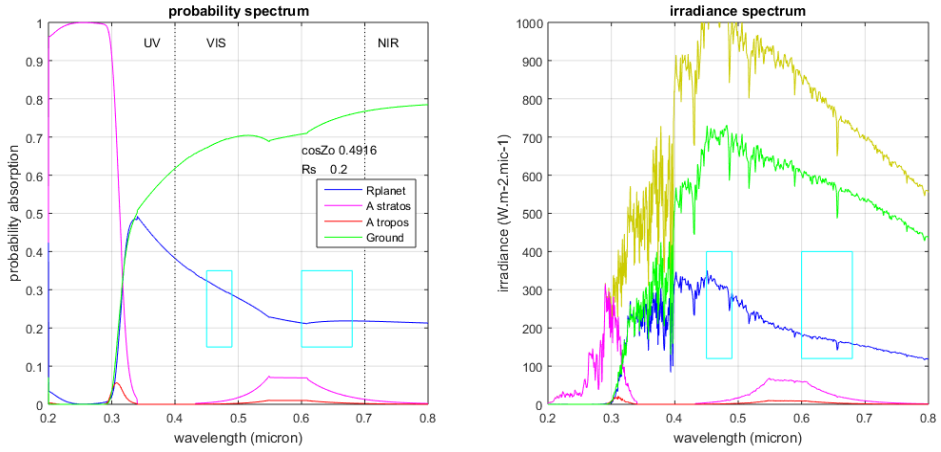

Figure 11. Spectral probabilities and absorbed irradiances in clear-sky conditions, Rs= 0.2, Z0~60º. Rectangles in cyan illustrate the spectral interval of ABI channels 1 and 2. Yellowish line: Extraterrestrial irradiance.

It is seen that

- Stratospheric Hartley band eliminates solar spectrum at λ<0.3 μm, leaving no irradiance to be allocated at troposphere, space or ground.
- Troposphere can be considered virtually conservative (with null absorption).
- UV contribution within 0.3-0.4 μm to space and ground irradiances is not negligible.
- Absorption in stratospheric Chappuis band is low but not negligible; it also shows some influence on spectral exit probability but not on associated irradiance.

Figures 12 illustrate the influence of spectrally variable ground reflectance *Rs*(λ) (shown in figure 7).

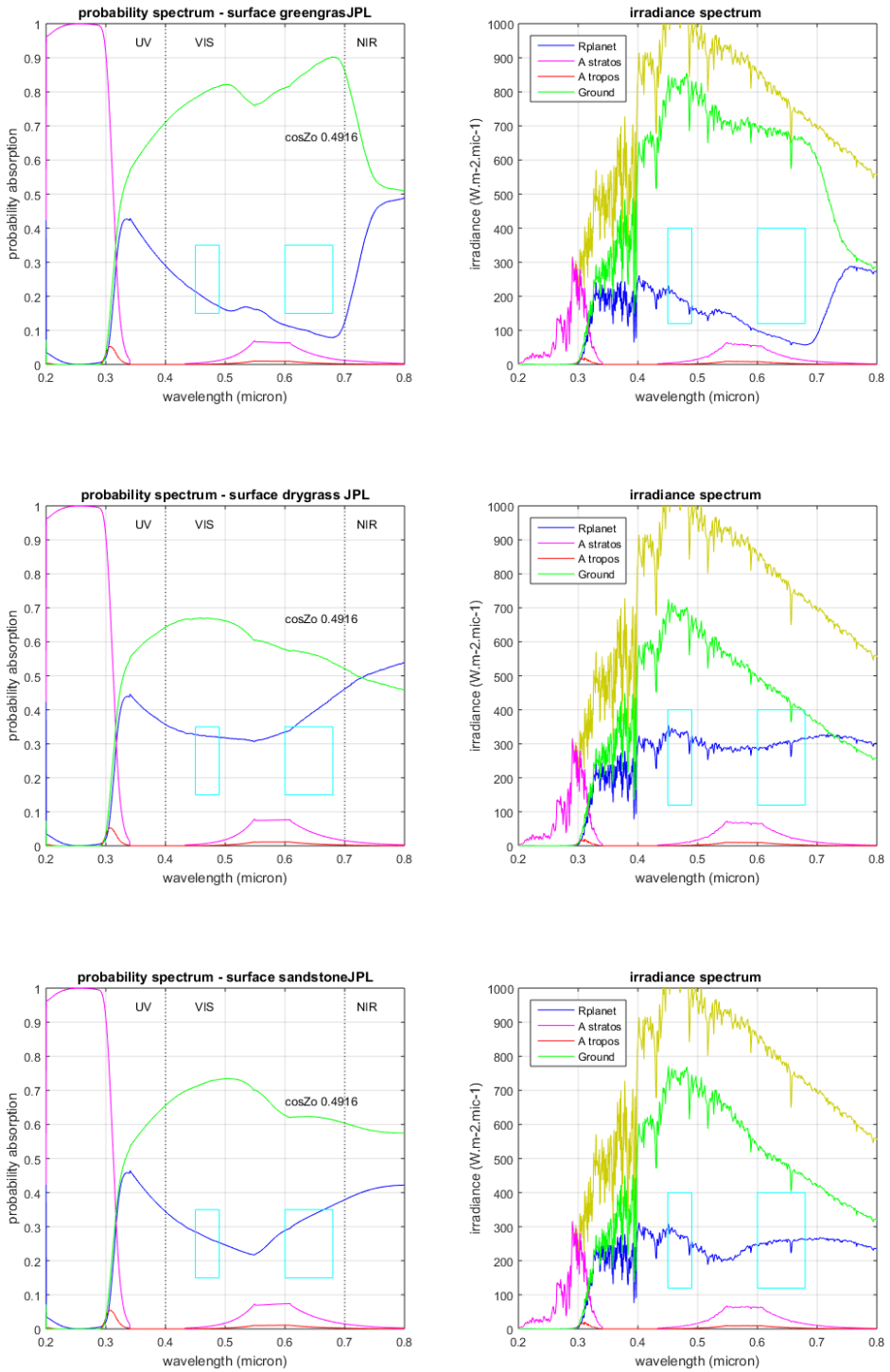

Figure 12. Spectral probabilities and absorbed irradiances in clear-sky conditions, Z0~60º for three types of surface. Rectangles in cyan illustrate the spectral interval of ABI channels 1 and 2. Yellowish line: Extraterrestrial irradiance.

When considering Rs varying with λ, irradiances of regions r=1, 2, 3, 4 in UVNIR interval have been referred to TOA UVNIR:

$$\text{DeltaS}_o = \Sigma_{UVNIR}\, S_{oi}\, \delta\lambda_i\,, \tag{5.6a}$$

$$E(r, \mu_o) = \Sigma_{UVNIR}\, \pi(r, \mu_o, \lambda_i)\, S_{oi}\, \delta\lambda_i \;/\; \text{DeltaS}_o\,, \tag{5.6b}$$

$$G(\mu_o) = \Sigma_{UVNIR}\, [\pi(4, \mu_o, \lambda_i)/(1\text{-}Rs_i)]\, .\, S_{oi}\, \delta\lambda_i \;/\; \text{DeltaS}_o \tag{5.6c}$$

Figures 13 show results in four types of surface characteristics.

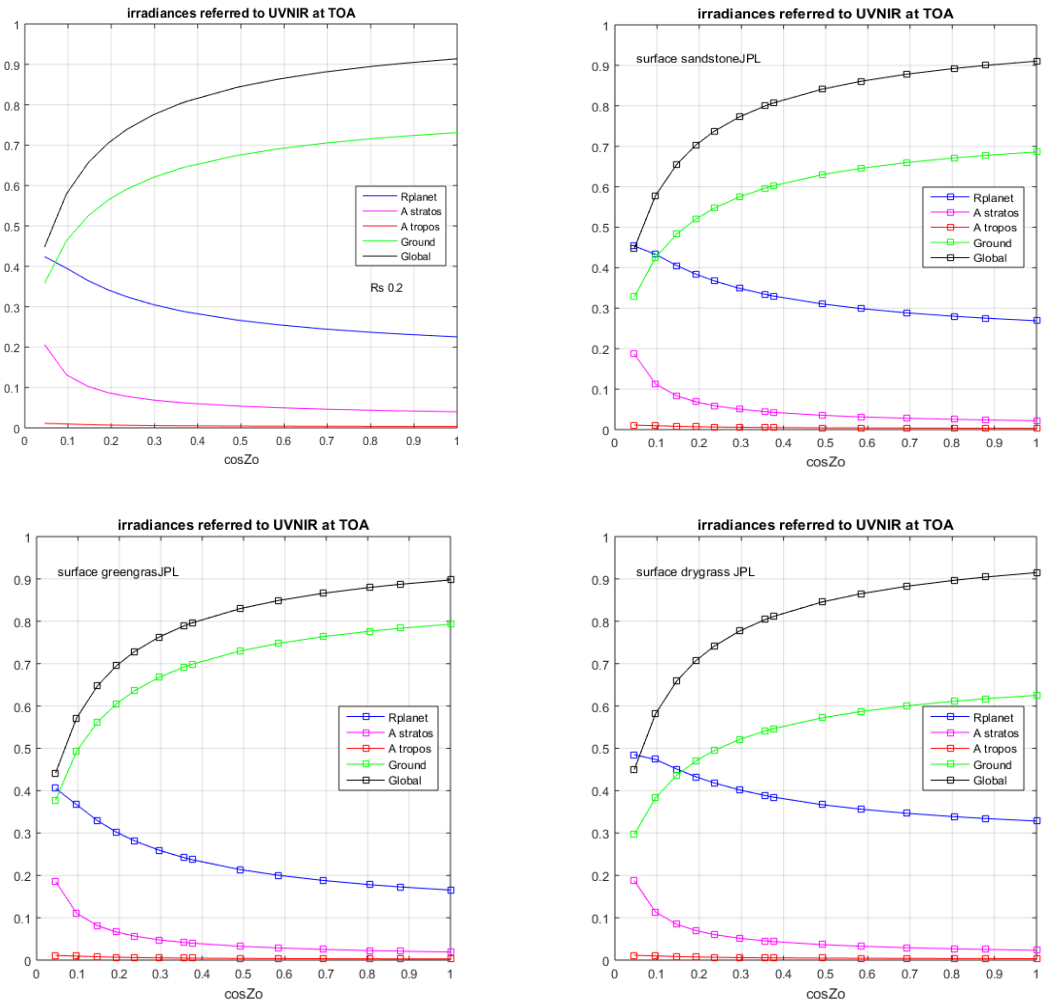

Figures 13. Exiting and absorbed irradiances (stratosphere, troposphere, ground) and global incident on surface, interval UVNIR, related to TOA irradiance.

5.4. RpUVVIS as a function of cosZo for several types of surface.

It is interesting to note that the set of relative fluxes in figures 13 have similar behavior, in despite of the variety of spectral characteristics illustrated in figures 12. Therefore, some simple parameterizations of planetary reflectance *Rp* could be fitted to STOCH2F results. Figure 14 shows behavior of *Rp*(UVNIR) with solar zenith angle Z_o, for six types of surface,

TROP atmosphere. It was found a fairly good fit (illustrated by crosses in figure 14, left) with the function

$$Rp = a \,/\, (1 + b\,\mu_o + c\,\mu_o^2) \qquad (5.8)$$

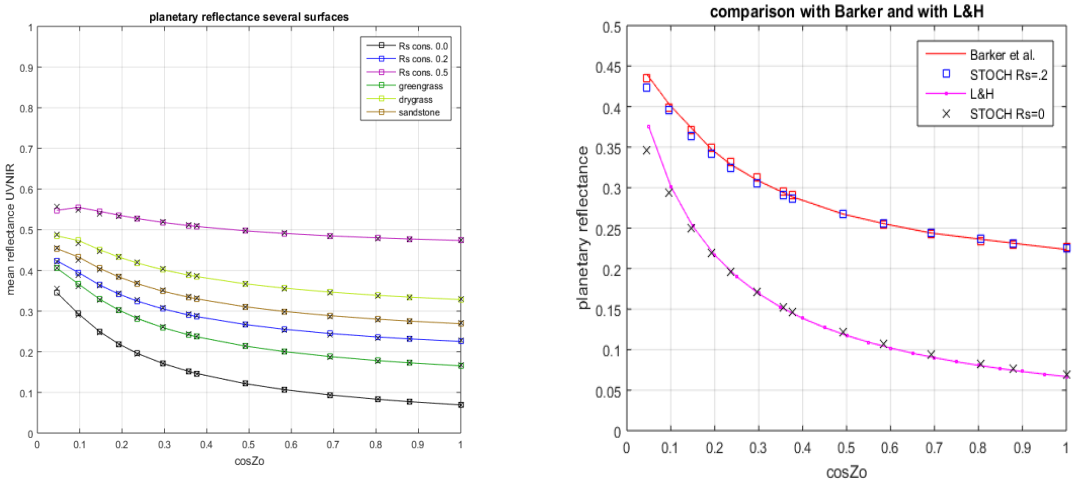

Figure 14. (*left*) Behavior of planetary reflectance *Rp*, UVNIR interval. (*right*) Comparison STOCH2F vs. two other estimates.

Table 3. Parameterizations of planetary reflectance *Rp* (mean value in UVNIR interval). Mean *Rs* is weighted in UVNIR interval with (1) incidence of white spectrum; (2) the first-impact irradiance on ground, μ_o=1.

Type of surface	Mean *Rs* (1)	Mean *Rs* (2)	*a*	*b*	*c*
Constant reflectance	0.00	0.00	0.441	5.313	0.052
	0.20	0.20	0.456	1.879	-0.874
	0.50	0.50	0.566	0.355	-0.160
greengrass			0.458	2.877	-1.126
drygrass			0.511	1.042	-0.494
sandstone			0.485	1.481	-0.694
Barker et al. UVVIS	0.20	0.20	0.474	2.027	-0.934
L&H adapted	0.00	0.00	0.495	6.430	0.0

Table 3 shows coefficients (*a b c*) obtained for fitting to STOCH2F results. The type of surface is characterized by spectrally constant reflectance (three cases), and vegetation or sandstone ground (three cases, see figure 7). A mean reflectance for *Rs* corresponds to a value weighted with irradiance impinging ground:

$$Rs(\text{mean}) = \int_{UVNIR} Rs(\lambda)\, G_{oo}(\lambda,\mu_o)\, d\lambda \;/\; \int_{UVNIR} G_{oo}(\lambda,\mu_o)\, d\lambda. \qquad (5.9)$$

For *Rs* mean values in Table 3, irradiance G_{oo} has been assumed 1) constant (white spectrum); 2) first-order impact of solar radiation on ground, be

$G_{oo}(\lambda, \mu_o) = [P_o(28) + \exp(-\tau/\mu_o)]\ \mu_o\ S_{o\lambda}$. (5.10)

Figure 14 (right) also shows two comparisons with other model results, namely Barker et al. (2003) and Lacis and Hansen (1974).

Barker et al. (2003) published an intercomparison of 25 1D codes from 19 participants, for clear-sky and overcast conditions. Specifications within solar spectrum were: McClatchey et al. (1972) tropical atmosphere, $0.05 \le \mu_o \le 1$, lambertian constant ground albedo $Rs = 0.2$, integrated wavelength interval 0.2-0.7 μm (here referred to as UVVIS). Table 3 shows coefficients using fitting function given by eq. (5.8), and figure 14 illustrates the fair coherence with STOC2F for $\mu o \ge 0.1$. For $\mu o = 0.05$ STOCH2F underestimates Barker's reflectance by 0.15 (~3%).

Lacis and Hansen (1974) reported the expression (declared accurate within 1%)

$Rp_{LH} = 0.28/(1 + 6.43\ \mu_o)$. (5.7)

Eq. (5.7) corresponds to total solar spectrum, black ground ($Rs = 0$), O_3 profile in MLW atmosphere, and U.S. Standard Atmosphere (21 layers). Calculation was performed using "adding method" code. It is worth to note that: 1) Rayleigh optical thickness is $\tau_R < 0.02$ for $\lambda > 0.8$ μm; 2) a black ground is assumed; therefore, $Rp(\lambda)$ may be assumed negligible outside UVNIR interval. This one accounts for 56.6% of solar constant (eq. 4.2); thus, an effective *Rp* value *referred to UVNIR* would need a correction factor $\gamma = 1/0.566 = 1.767$ so that $Rp_{LH}(\text{adapted}) = \gamma\ Rp_{LH}$. Figure 14 shows that STOCH2F ($Rs = 0$, $\mu_o > 0.1$) closely fits LH-based expression.

It is concluded that STOCH2F estimates and parameterizations of integrated $Rp(\mu_o, Rs)$ are fairly accurate for $\mu_o > 0.1$ (or $Z_o < 84.2^o$). An important point is that STOCH2F parameterization already includes the effects of O_3 absorption. For higher zenith angles, the plane-parallel hypothesis is no longer valid and two-flux model in STOCH2F should be adapted to actually spherical structure of atmosphere. This will be a future task of STOCH2F modeling.

Multiple reflections within atmosphere

Planetary reflectance *Rp* can be thought of in terms of the following sequence: 1) there is a first-time contribution $\pi_o(1)$ of random walk (consistent with ground reflectance $Rs = 0$); 2) a global radiation $G_o(\mu_o)$ impinges on this black ground; 3) given the actual value $Rs > 0$, a fraction *Rs* of G_o generates diffuse upward photons at state 29; 4) atmosphere has an intrinsic transmittance T^* and a counter-reflectance R^*; 5) multiple reflections on ground and successive transmittances create contributions $\pi_n(1)$ to a total reflectance $\pi(1)$. The corresponding algorithm is

$\pi_o(1) = \pi(1, Rs = 0);\ G_o = \pi(2, Rs = 0);$ (5.8a)

$\pi_1(1) = G_o\ Rs\ T^*,$

$\pi_2(1) = (G_o\ Rs).(R^*\ Rs).T^* = \pi_1(1) . (R^* Rs),$

…

$\pi_n(1) = \pi_{n-1}(1) . (R^* Rs) = G_o\ Rs\ T^*.(R^*\ Rs)^{n-1};$

$\pi(1) = \Sigma_n\ \pi_n = \pi_o(1) + G_o\ Rs\ T^* / (1 - R^*\ Rs).$ (5.8b)

Eqs. (5.8) make evident that (R*, T*) are fundamental parameters for describing planetary reflectance. They are found applying STOCH2F code to the multilayered atmosphere, with initial vector P_o being null except for $P_o(29)= 1$, and $Rs= 0$ (equivalent to state Q(28,29)=0, Q(28,2)=1 in transition matrix).([9]). Figure 15 shows the results; it is seen that model algorithm of eqs. (5.8) yields the same original spectral $Rp(\lambda)$. It is interesting to note that

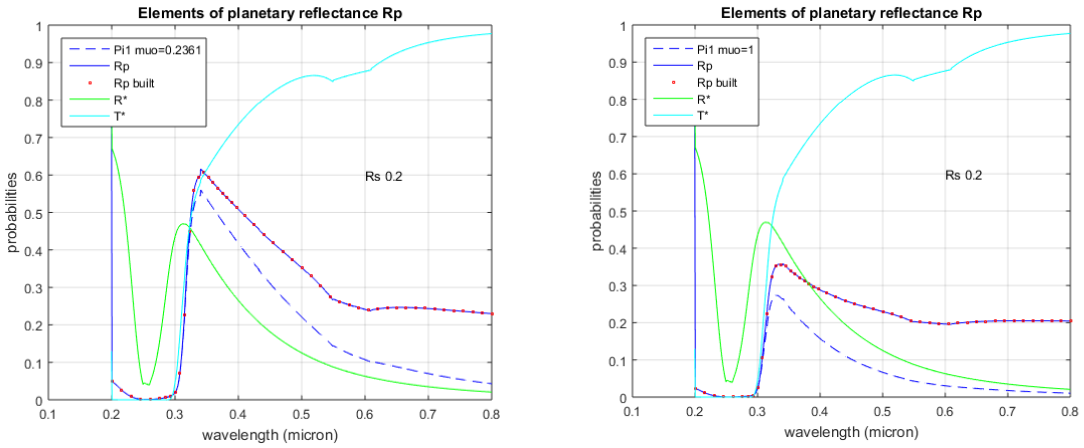

Figure 15. Elements of *Rp* composition, for two zenith angles (μo= 0.236 and 1.000). Ground reflectance *Rs*= 0.2 , TROP atmosphere.

- Counter-reflectance *R** and transmittance *T** for diffuse photons are independent of ground reflectance *Rs*;
- Exiting $Rp(\lambda)$ for $\lambda \leq 0.3$ μm can be discarded. Ozone does not allow transmission of upward diffuse radiance, and somewhat high values of R* are actually produced by backscattering processes below the stratosphere. In addition, figure 12 shows that solar flux on TOA is not intense enough and associated flux to $\pi(1)$ is negligible.
- Contribution of UV in Δ:(0.3-0.4) μm, together with increasing $S_{o\lambda}$ values, is not negligible. It is mainly due to scattering processes: $\pi_o(1) \sim \pi(1)$; in VIS spectrum, main contribution is due to multiple reflections and $\pi_o(1) << \pi(1)$ at $\lambda > 0.6$ μm.
- Satellite observations of clear-sky pixels will be "bluished" in a channel centered at 0.48 μm, while a channel at 0.65 μm will observe near real values of *Rs*. However, for higher Z_o atmospheric scattering can increase by 25% the real *Rs* value.

[9] *R** is the probability of return from ↑ to ↓ at the same level *z*=0 after a random walk through the entire atmosphere, including partial absorption by O_3.

5.5. A model for clear-sky irradiance at ground level in UVNIR interval

Figures 16 illustrate different characteristics of clean clear-sky black-ground components of solar fluxes within atmosphere. They show that spectral G has a somewhat complex behavior, in probability as well as in radiative flux terms.

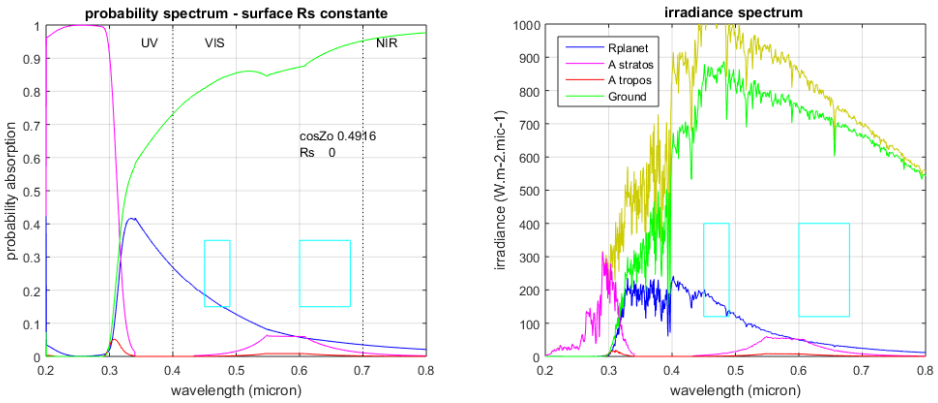

Figure 16. Spectral characteristics of main radiative variables Rplan, A (stratosphere), A (troposphere), Ground absorption, in terms of probabilities and of fluxes. Z_o=60º, Rs=0.

Similarly to algorithm in eqs. (5.8), irradiance G could be evaluated in terms of multiple reflections after initial value G_o= $G(\lambda, \mu_o, Rs=0)$, leading to a total global irradiance $G(\lambda, \mu_o, Rs)$

$$G= G_o + G_o\, Rs\, R^* + G_o\, (Rs\, R^*)^2 + \ldots = G(\lambda, \mu_o, Rs=0) \,/\, (1 - R^*\, Rs). \qquad (5.9)$$

The mean value over UVNIR interval is

$$G(\text{mean})= \int_{UVNIR} G_o\, S_{o\lambda} \,.\, (1-R^*\, Rs)^{-1}\, d\lambda \,/\, S_{oUVNIR}. \qquad (5.10)$$

Even with Rs being constant, R^* is a function of λ and the integral in (5.10) is not straightforward. At least for the case Rs=constant, it could be defined a weighted mean value R^{**} of R^*, such that

$$G(\text{mean})= G_o(\text{mean}) \,/\, (1- R^{**}\, Rs). \qquad (5.11)$$

It could be expected that dependence of G_o on incident angle Z_o induce some R^{**} variability. STOCH2F code was used to generate spectrally integrated G for a variety of values of Z_o and Rs. Figure 17 shows that R^{**} has a rather constant value, varying from R^{**}~0.134 for Z_o<60º to R^{**}~0.119 for Z_o>76º. Lacis and Hansen (1974) reported the value $R_{LH}{}^{**}$= 0.0685 for atmospheric counter-reflectance over the entire solar spectrum and averaged over all zenith angles. Following the same argument of nearly null scattering over

0.8 μm (used for adapting eq. 5.7) the corrected value for UVNIR interval would be γ R_{LH}**= 0.121, fully compatible with our STOCH2F. In addition, linearity in figure 18 suggests low dependence of *R*** on *Rs even if this one is spectrally variable* (like in vegetation surfaces).

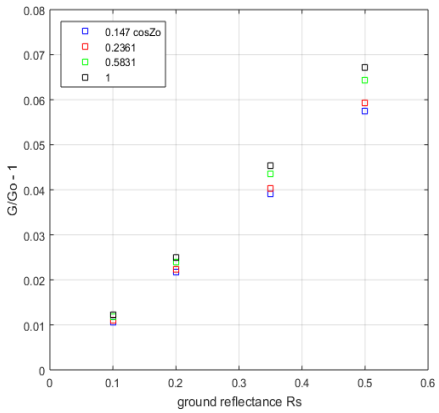

Figure 17. Evidence of near constant values of *R*** (eq. 5.11)

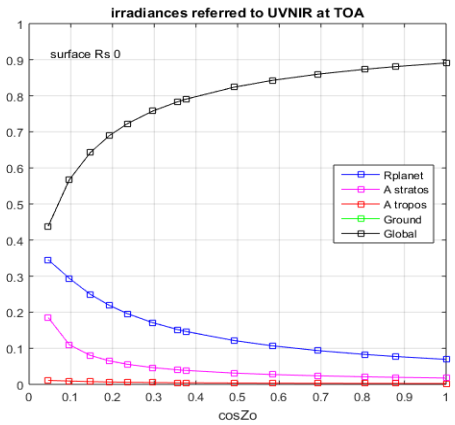

Figure 18. Components of solar radiation absorption for *Rs*=0.

Parameterization of $G_o(\mu_o)$ would complete modeling in eq. (5.11). Instead of tempting a parameterization of Go itself, it is interesting (and simpler) to consider a radiative balance in UVNIR interval (see figure 18):

$$Rp + A_{stratos} + A_{tropos} + G_o/(1- R^{**} Rs) = 1, \qquad (5.12)$$

and irradiance *GL* in $W.m^{-2}$ is (well understood: *Rp*, *A*, G_o refer to integrated probabilities over UVNIR),

$$GL = \mu_o S_{UVNIR} (1 - Rp - A) /(1 - R^{**} Rs). \qquad (5.13)$$

Similar reasoning was presented in Ceballos (2000), with simplifying hypotheses (constant *Rs*= 0.06-0.08 , *A*= 0). Reflectance *Rp* may be parameterized following eq. (5.8) and some basic information about surface characteristics. The point is: *can be the absorption term A disregarded*?

Certainly, tropospheric absorption by O_3 can be disregarded, but *A*(stratos) eventually not, especially for μ_o<0.3 (Z_o>72º), see figures 13 and 18. A set of STOCH2F results (*Rs*= 0, 0.1, 0.2, 0.35, 0.5) was analyzed, finding a fitting function

$$A_{stratos}(\mu_o, Z_o) = f . A_o(\mu_o, Rs=0),$$

$$A_o= 0.3204 / (1+20.53\ \mu_o - 3.36\ \mu_o^2), \qquad f= 1 + 1.1\ Rs\ \mu_o . \qquad (5.14)$$

Eq. (5.13) together with (5.8) for *Rp* and (5.14) for $A_{stratos}$ yield a model for global insolation *GL* in a clear-sky TROP atmosphere, spectral interval UVNIR:(0.2-0.8 μm).

6. Final considerations

Stochastic point of view provides an useful tool for diagnostic analysis of radiation transfer in atmosphere, allowing detection and quantification of the main processes and atmospheric parameters having influence.

In this chapter, a plane-parallel 13-layered atmosphere was considered, in spectral interval UVNIR:(0.2-08 μm) with typical profiles of McClatchey et al. (1972). Stochastic scheme consist of a random walk of diffuse photons from an initial state until an absorbing one (within a layer, at ground or at outer space). The process is actually a first-order Markov chain, with transition probabilities defined by reflectance, absortance and transmittance for diffuse photons, assessed by the solutions of the usual two-flux RTE.

Clean clear-sky case was considered, where ozone absorption and Rayleigh scattering are the acting processes. Thirteen layers and 2-flux Eddington scheme have been enough build a stochastic scheme showing main aspects of radiative transfer. Five examples of application were developed, leading to a better understanding of some transfer processes.

Parameterizations of planetary reflectance and atmospheric absorptance are accuratelt described. A better description is needed for very low inclination angles.

The final example developed a model for global radiation in UVNIR interval. It is an enhanced version of the GLo simplified version for UVVIS interval (Ceballos 2000), currently in use in various applications at Satellite Division `DISSM/CGCT/INPE`.

The next chapters will consider more complex situations, as non-Beer law behavior of H_2O and CO_2 absorption, and interaction of solar radiation with aerosol and cloud multilayered atmosphere.

The STOCH2F code is primarily written in MatLab language, compatible with Octave. Further adaptation to Python will be accomplished. It is expected to build a standardized STOCH code useful for teaching and research of radiative phenomena in Eart-atmosphere system.

Appendix A

Two-flux solutions for a layer

For an homogeneous layer, diffuse irradiances are solutions of a pair of linear differential equations

$$dE\downarrow/d\tau = -a_1\, E\downarrow + a_2\, E\uparrow + a_5\, \omega\, \Phi \qquad (4)$$

$$dE\uparrow/d\tau = -a_3\, E\downarrow + a_4\, E\uparrow + a_6\, \omega\, \Phi.$$

These equations arise from different approaches for RTE solutions. Popular examples in the literature are the SS-approximation of Coakley and Chylek (1975), the Eddington (EDD-) approximation found by Shettle and Weinman (1970), and the two-stream method of Liou (2002). The first one assumes isotropic radiances $L\uparrow$ and $L\downarrow$, thus $E\uparrow\downarrow = \pi\, L\uparrow\downarrow$. Eddington approximation considers a first order Legendre polynomial approximation $L = a + b\, P_1(\mu)$, $\mu = \cos Z$, for ascending and for descending radiances. Liou's method comes from a complex solution of RTE which describes the radiation field with N ascending plus N descending radiances; it considers the approximation $N=1$. Ceballos (1988) and Zdunkowski et al (2007) have analyzed the common aspects of these approximations, the relationship between a_1-a_4 coefficients and the structure of diffuse radiance.

Section 4.5 defined parameters *bmed* and *mumed*. For SS- and EDD- approximations, the coefficients a_1-a_6 in eqs (4) are defined by (Ceballos 1986, 1988: Zdunkowski et al. 2007, ch. 6)

$$a_1 = [1 - \omega(1- bmed\downarrow)]/mumed\downarrow - Edd \qquad a_2 = \omega\, bmed\uparrow/mumed\uparrow - Edd \qquad (A.1)$$

$$a_3 = \omega\, bmed\downarrow/mumed\downarrow - Edd, \qquad a_4 = [1 - \omega(1- bmed\downarrow)]/mumed\downarrow - Edd,$$

$$a_5 = 1 - b_o, \qquad a_6 = - b_o.$$

- For the mixture ar+O_3 triads are $\{\tau = \tau_R + \tau_3,\ \omega = \tau_R/\tau,\ g = 0\}$.
- Parameters *mumed* are averages of $\mu = \cos Z$ assessed in the same sense that eq (14b). We have $mumed\uparrow\downarrow = 1/2$, $bmed\uparrow\downarrow = 1/2$.
- Edd=0 for SS- and Edd=1/4 for EDD-approximation.

Two-flux solutions for individual N layers

We adopt approximations SS (`Edd=0`) or EDD (`Edd=.25`). Variable `Triads` has components (τ,ω,g) in Ncam layers.

1) Direct incidence

```
function [Ro, To, Ao, Too] = f2Fdiro(muo, Triads, Edd)
% calcula parametros de transmissao de rad direta nas Ncam camadas
% Não aplica correcao Rodgers

[Ncam, Nparam]= size(Triads); mo= 1/muo;
fator= ones(Ncam,1);
rodgers=0;
Mr= 35/sqrt(1224*muo*muo+1); Mo=1;
fator=M*(rodgers==0) + Mr*(rodgers==1);
moo= fator*mo;
```

```
Ro= zeros(1,Ncam); To= zeros(1,Ncam); Ao= zeros(1,Ncam); Too= zeros(1,Ncam);
taus= Triads(:,1); omegas= Triads(:,2);gs= Triads(:,3);
for cam=1:Ncam
    omega= omegas(cam); tau= taus(cam); g= gs(cam);
    bm= (1-3*g/4)/2; mum=1/2; bo= (1- 3*g*muo/2)/2;
        a1= (1- omega*(1-bm))/mum - Edd;  a2= omega*bm/mum - Edd;
        a3= a2; a4= a1;
        a5= 1- bo; a6= -bo;
    omegabaixo= .1; taumuitobaixo=.1;
    tauo= moo*tau;
    if tauo<=taumuitobaixo;
        Tdir= 1- tauo; Ab= tauo*(1-omega);
        T= tauo*omega*(1-bo); R= tauo*omega*bo;
    end
    if tauo> taumuitobaixo
        if omega==1    %atmosfera conservativa: omega==1
            alfa= a2;
            R= (alfa*tau -(alfa*muo- bo)*(1- exp(-tauo)))/ (1+alfa*tau);
            Tdir= exp(-tauo);
            Ab=0; T= 1- Tdir - R;
        else
            % solucao particular (condicao: omega>0)
            Delta= mo*mo + a2*a2-a1*a1;
            Bd= mo*omega*(-a5*(mo+a4)+a2*a6)/Delta;
            Bu= mo*omega*(-a6*(mo-a1)-a5*a3)/Delta;
            % solucao homogenea
            gama=  sqrt(a1*a1 - a2*a2);
            alfa1= (a1-gama)/a2; alfa2= (a1+ gama)/a2;
            % aplica condicao contorno para solucao completa
            to= exp(-moo*tau);
            t= exp(-gama*tau);
            Delta1= alfa2/t - alfa1*t;
            A1= (Bu*to- Bd*alfa2/t)/Delta1;
            A2= (-Bu*to+ Bd*alfa1*t)/Delta1;

            R= alfa1*A1+ alfa2*A2 + Bu;
            T= A1*t + A2/t +Bd*to;
            Tdir= to; Ab= 1- Tdir- T -R;
         end
    end
    To(cam)= T; Ro(cam)= R; Ao(cam)= Ab; Too(cam)= Tdir;

end  %end funcao
```

2) Diffuse incidence

```
function [Rd, Td, Ad] = f2Fdif(Triads, Edd)
%calcula parametros de transmissao de rad difusa numa camada

[Ncam, Nparam]= size(Triads); DDif= 5/3;
%DDif=1.9;  %Lacis & Hansen 1974, não aplicado
Rd= zeros(1,Ncam); Td= zeros(1,Ncam); Ad= zeros(1,Ncam);
taus= Triads(:,1); omegas= Triads(:,2); gs= Triads(:,3);
for cam=1:Ncam
    omega= omegas(cam); tau= taus(cam); g= gs(cam);
    omegabaixo= .05;
    if omega<omegabaixo
       T= exp(-DDif*tau); R= 0; Ab= 1-T;
    end
    if omega>= omegabaixo
       bm= (1-3*g/4)/2; mum=1/2;

    if omega==1
        omega=.9999;
    end
```

```
    b= (1 - 3*g/4)/2; mu= .5;
    a1= (1-omega*(1-b))/mu -Edd; a2= omega*b/mu -Edd;
    gama= sqrt(a1*a1 - a2*a2);
    beta1= (a1- gama)/a2; beta2= (a1+ gama)/a2;
    U= ones(2);
    U(2,1)= beta1*exp(-gama*tau); U(2,2)= beta2*exp(gama*tau);
    B= U\[1; 0]; B1= B(1); B2= B(2);
    R= beta1*B1 + beta2*B2;
    T= B1*exp(-gama*tau)+ B2*exp(+gama*tau);
    Ab= 1 - R - T;
  end
    Td(cam)= T; Rd(cam)= R; Ad(cam)= Ab;

end  %end do loop N camadas

end  %end funcao
```

Appendix B

Some basic subroutines and the SOCH2F algorithm

Applying model STOCH2F

```
% ================================================= aplica Stoch
lamda= lamdauvnir; %mu= muP;
[TriadN, PiN, Poo, Pio, W]= fSpectralStocho(mu, X, lamda, Rs, Edd);
P= PiN(:,1:end-1,:); Pitrans= squeeze(PiN(:,end,:));
%PiN(Nlam,Ncam+3,Nmu)
Po= Poo(:,1:NPis,:);  %Poo(Nlam,NE,Nmu)
Rx= W(:,1); Rxe= W(:,2); Tx= W(:,3); Txe= W(:,4);
Rx1= W(:,5); Rxe1= W(:,6); Tx1= W(:,7); Txe1= W(:,8);
Rpo= squeeze(Pio(:,1,:)); GLo= squeeze(Pio(:,2,:));
% ================================================ fornece PIS e TriadN
```

Ncam	number of layers
NA = Ncam+2	number of absorbing states
NE= 3*Ncam+2	number of states

Input:

`mu [Nmu, 1]`	Nmu values of cos Zo
x `[Ncam+1, 5]`	Atmospheric structure (see Table ...)
`lamda [Nlam, 1]`	Nlam values of wavelength
`Rs [Nlam, 1]`	ground reflectance
`Edd [1, 1]`	coefficient for SS or EDD approximation

Output:

`TriadN [Ncam, 3]`	{τ ω g}
`PiN [Nlam, Ncam+3, Nmu`	final probabilities [Nlam Ncam+3 Nmu]
`Poo [Nlam, NE, Nmu]`	probabilities of first allocation in NE states
`Pio [Nlam, NA, Nmu]`	probabilities of absorption, Rs=0.
`W [Nlam, 8]`	Diffuse reflectance and transmittance of troposphere and stratosphere, black and non-black surface

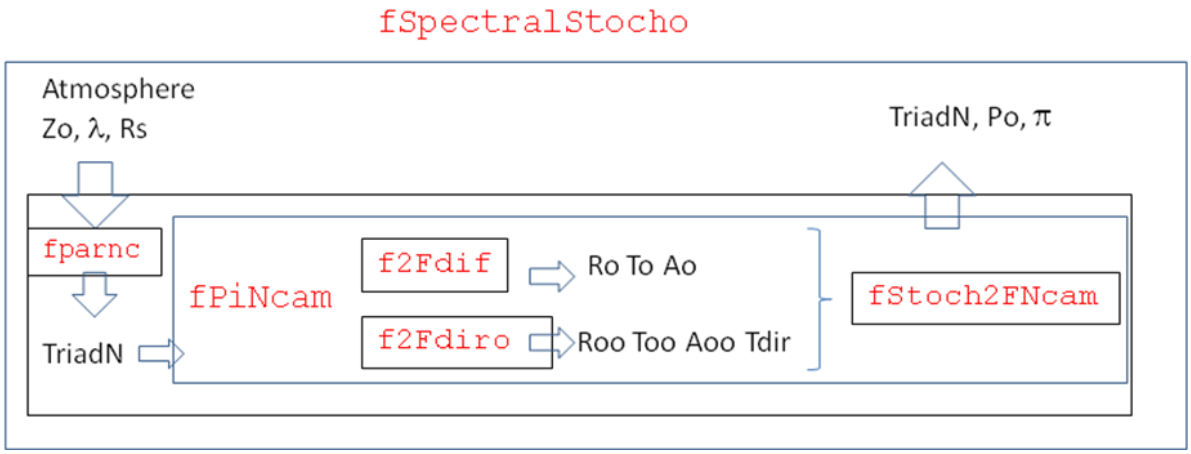

function fPiNcam

```
function [PiN, Po, Pio,W] = fPiNcam(lamda, muo, TriadN, zbase, Edd, Rs)
%Recebe perfil da atmosfera + refletancia solo
%Entrega perfil absorcao + refletancia difusa atmosfera e
%estratosfera (Ncam+4 colunas) em Nlamda linhas do espectro solar

% ========== probabilidades de estado=======================
% estado inicial: indicar qual estado como Eo
% para incidência de rad direta, indicar Eo=ZERO
% NQ indica a potencia esperada para Q

[Nlam, Ncam, Ntri]= size(TriadN);
NQ= 50; NE= 3*Ncam+2; NA= Ncam+2;
Uo= zeros(Nlam,1);
Pi= zeros(Nlam, NE);
Rx= Uo; Rxe= Uo; Tx= Uo; Txe= Uo; Pitrans= Uo;
Rx1= Uo; Rxe1= Uo; Tx1= Uo; Txe1= Uo;
Po= zeros(Nlam, NE); Pioo= zeros(Nlam,NA);
X= zeros(Ncam,7, Nlam);  %propriedades de transferencia das camadas

for L=1:Nlam
    % ========================================================
    LL= lamda(L); Rs= Rss(L);
    tau= squeeze(TriadN(L,:,1));
    omega= squeeze(TriadN(L,:,2));
    g= squeeze(TriadN(L,:,3));

    Eddif=0;
    [R, T, A]= f2Fdif(tau, omega, g, Eddif);
    A= A.*(A>0)+ 1e-5*(A<=0);
    Rd= R; Td= T; Ad= A;

    [R, T, A, Tr]= f2Fdiro(muo, tau, omega, g, Edd, zbase);
    A= A.*(A>0)+ 1e-5*(A<=0);
    Ro= R; To= T; Ao= A; Tdir=Tr;
    if teste==3
        X(:,:,L)= [Tdir; To; Ro; Ao;  Td; Rd; Ad]';
    end
    % ========================================================
    AA= Ad; RR= Rd; TT= Td;
    AAo= Ao; RRo= Ro; TTo= To; TTdir= Tdir;

    Eo= 0;  %incidencia direta
    PQL= fStoch2FNcam(Eo,NQ, Rs, Ad,Rd,Td, Ao,Ro,To,Tdir);
    Pi(L,:)= PQL(end,:);     %NQ produtos, NE estados, lamda
    Pitrans(L)= sum(Pi(L,Ncam+3:end),2); Po(L,:)= PQL(1,:);
    % -------------------- incidencia direta solo preto
    Eo=0; Rso=0;
    PQL= fStoch2FNcam(Eo,NQ, Rso, Ad,Rd,Td, Ao,Ro,To,Tdir);
    Pioo(L,:)= PQL(end, 1:NA);
    %---------------------- contrarref atmosfera
    Eo=2*Ncam+3; %estado ascendente no solo
    Rso= Rs;
    PQL= fStoch2FNcam(Eo,NQ, Rso, Ad,Rd,Td, Ao,Ro,To,Tdir);
    Rx1(L)= PQL(end,2); %absorcao normal no solo
    Tx1(L)= PQL(end,1); %transmitancia com reflexao do sol
    Rso=0;
    PQL= fStoch2FNcam(Eo,NQ, Rso, Ad,Rd,Td, Ao,Ro,To,Tdir);
    Rx(L)= PQL(end,2); %contrarrefletancia atmosferica
    Tx(L)= PQL(end,1); %transmitancia da rad. refletida
```

```
    % -------------------- contrarref estatosfera
    camcega= 10; nupcega= NE- (camcega-2);
    Eoup= nupcega; %estado ascendente em 16km
    Rso= Rs;
    PQL= fStoch2FNcam(Eoup,NQ, Rso, Ad,Rd,Td, Ao,Ro,To,Tdir);
    Rxe1(L)= PQL(end,2); %absorcao normal no solo
    Txe1(L)= PQL(end,1); %exir incluindo reflexao no solo
    Rso=0;
    AAe = AA; RRe=RR; TTe=TT;
    %RRe(camcega+1)=0; AAe(camcega+1:end)= 0; TTe(camcega+1:end)= 1;
    RRe(camcega:end)=0; AAe(camcega:end)= 0; TTe(camcega:end)= 1;
    PQL= fStoch2FNcam(Eoup,NQ, Rso, AAe,RRe,TTe, AAo,RRo,TTo,TTdir);
    Rxe(L)= PQL(end,2); %contrarrefletancia estratosfera
    Txe(L)= PQL(end,1); %upward transmittance da estratosfera
end
W= [Rx Rxe Tx Txe Rx1 Rxe1 Tx1 Txe1];
PiN= [Pi(:, 1:Ncam+2), Pitrans];

end    %end function
```

function fStoch2FNcam

```
function P= fStoch2FNcam(Eo,NQ, Rs, A,R,T, Ao,Ro,To,Tdir)
%Fornece probabilidades de estado finais em 11 camadas

% ESQUEMA11cam = ...
%
%     {'        O 1         ';
%     '--------------------       70 km';
%     '        O 3         cam 1';
%     '-35--^--------v-14--       50 km';
%     '        O 4         cam 2';
%     '-34--^--------v-15--       40 km';
%     '        O 5         cam 3';
%     '-33--^--------v-16--       35 km';
%     '                    ';
%     ' ................. ';
%     '        O 11        cam 9';
%     '-27--^--------v-22--       06 km';
%     '        O 12        cam10';
%     '-26--^--------v-23--       03 km';
%     '        O 13        cam11';
%     '_25__^________v_24________ 00 km';
%     '/////// O 2 ///////////////'}

Ncam= length(A);
NE= 3*Ncam+2; %NE= numero de estados
NA= Ncam+2; %numero estados absorventes
Q= zeros(NE, NE); Q(1:NA,1:NA)= eye(NA);

%incidencia de direta no topo
%camada 1
Q(NE, 1)= T(1); Q(NE, 3)= A(1); Q(NE, NA+1)= R(1);
% 2:Ncam camadas
for cam=2:Ncam
    desce=NA+cam-1; sobe= (3*Ncam+2)-(cam-2);
    Q(desce, sobe)= R(cam);
    Q(desce, desce+1)= T(cam);
    Q(desce, cam+2)= A(cam);
    Q(sobe-1, sobe)= T(cam);
    Q(sobe-1, desce+1)= R(cam);
    Q(sobe-1, cam+2)= A(cam);
end
%base
Q(NA+Ncam,2)= 1-Rs; Q(NA+Ncam, NA+Ncam+1)= Rs;
```

```
Po= zeros(1,NE);
if Eo==0   %incidencia direta no topo
  TT=1;
  for cam=1:Ncam
    desce= NA+cam;
    sobe= (cam==1)+ (NE-cam+2)*(cam>1);
    Po(desce)= TT*To(cam); Po(sobe)= TT*Ro(cam); Po(cam+2)= TT*Ao(cam);
    TT= TT*Tdir(cam);
  end
    Po(2)= TT*(1-Rs); Po(NA+Ncam+1)= TT*Rs;
end

if Eo>0
    Po(Eo)=1;   %caminho estocastico comeca difuso em Eo
end
% -------------------------

P= zeros(NQ,NE);
P(1,:)=Po;   %radiacao original
for n= 2:NQ
    P(n,:)= P(n-1,:)*Q;
end

end   %end function
```

function fSpectralStocho

```
function [TriadN,PiN,Po,Pio,W]= fSpectralStocho(mu, X, lamda, Rs, Edd)
%recebe perfil atmosfera + lamdas, fornece Pis
%inclui contrarref atmosferica
 deltap= X(:,4)- X(:,3);
 ztopo= X(:,1); zbase= X(:,2); deltaz= ztopo-zbase;
 ptopo= X(:,3); pbase= X(:,4);
 MO3= 48; NAvog=6.02e23;
 NO3= X(:,5)*1e-5*(NAvog/MO3); %molec.m-3
 NO3= 1e-6*NO3;                %molec.cm-3

 %[O3]= 1.3E-5 em 40-50km segundo mcclatchey
Ncam= length(deltap); NPis= 2+Ncam; NE= 3*Ncam+2; Nmu= length(mu);
% ------------------------------------
Nlam= length(lamda);
Uoo= zeros(Nlam, Ncam); taucam= Uoo; omegacam= Uoo; gcam= Uoo;
TriadN= zeros(Nlam,Ncam, 3);
for L=1:Nlam         %calcula Triada
    LL= lamda(L);
    [tau, omega, g] = fparnc(LL,deltap, deltaz, NO3, zbase);
    taucam(L,:)= tau; omegacam(L,:)= omega; gcam(L,:)= g;
    TriadN(L,:,1)= tau; TriadN(L,:,2)= omega; TriadN(L,:,3)= g;
end
% ------------
PiN= zeros(Nlam,Ncam+3,Nmu); W= zeros(Nlam,2); Po= zeros(Nlam,NE,Nmu);
for nmu= 1:Nmu
    muo= mu(nmu);
    disp(['cosZo = ' num2str(muo)]);
 [PiN1,Po1, W] = fPiNcam(lamda, muo, TriadN, zbase, Edd, Rs);
 PiN(:,:,nmu)= PiN1; Po(:,:,nmu)= Po1;
end     %Ciclo de probabilidades finais

end
```

References.

Baldridge, A.M., S.J. Hook, C.I. Grove, G. Rivera (2009). The ASTER spectral library version 2.0. *Remote Sensing of Environment*, v. 113:711-715.

Barker, H.W., J.A. Davies (1992). Cumulus cloud radiative properties and the characteristics of satellite radiance wavenumber spectra. R. Sensing of Environment v. 42(1), 51-64.

Barker, H.W., Stephens, G.L., Partain, P.T., Bergman, J.W., Bonnel, B., et al. (2003). Assessing 1D atmospheric solar radiative transfer models: Interpretation and handling of unresolved clouds. *J. of Climate* 16, 2676-2699.

Bodhaine, B.A., N.B. Wood, E.G. Dutton, J.R. Slusser (1999). On Rayleigh optical depth calculations. *J. Atmos. Ocean. Technol*. v. 16:1854-1861.

Ceballos, J.C. (1986). *Um modelo estocástico de propagação da radiação solar na atmosfera* (A stochastic model for solar radiative transfer in the atmosphere). PhD Thesis, Instituto Astronômico e Geofísico, Universidade de São Paulo. 376 pp.

Ceballos, J.C. (1988). On two-flux approximations for shortwave radiative transfer in the atmosphere. *Contributions to Atmospheric Physics*, v. 61:10-22.

Ceballos, J.C. (1989). Stochastic properties of two-flux shortwave radiative transfer in the atmosphere. *Contributions to Atmospheric Physics* v. 62:180-192.

Ceballos, J.C. (2000). Estimativa de radiação solar à superfície com céu claro: Um modelo simplificado ("A simplified model for the assessment of clear sky solar irradiance at ground level"). *Rev. Brasil. de Meteorologia* v. 15(1):113-122.

Coakley, J.A., P. Chylek (1975). The two-stream approximation in radiative transfer: Including the angle of the incident radiation. *J. Atmos. Sci*. v. 32, 409-418.

Cox, D.R., H.D. Miller (1965). *The theory of stochastic processes*. Chapman and Hall, London.

Gueymard, C.A. (2004). The sun's total and spectral irradiance for solar energy applications and solar radiation models. Solar Energy v. 76(4):423-453 (doi: 10.1016/j.solener.2003.08.039)

Kargin, B.A., S.M. Prigarin (1994). Imitational simulation of cumulus clouds for studying solar radiative transfer in the atmosphere by the Monte Carlo method. *Atmos. Oceanic. Opt*. v. 7(9), 690-696.

Lacis, A.A., J.E. Hansen (1974). A parameterization for the absorption of solar radiation in the Earth's atmosphere. J. Atmos. Sci. v.31, 118-133.

Liou, K.N. (2002). *An introduction to atmospheric radiation*. Academic Press, 2nd Ed., 577 pp.

Mayer, B. (2009). Radiative transfer in the cloudy atmosphere. *Eur. Phys. J. Conferences* v. 1, 75-99 (doi: 10.1140/epjconf/e2009-00912-1).

McClatchey, R.A., R.W. Fenn, J.E.A. Selby, F.E. Volz, J.S. Garing (1972). *Optical properties of the atmosphere*, Third Ed. Air Force Cambridge Research Laboratories, Environ. Res. Papers No 411.

Meador, W.E., W.R. Weaver (1980). Two-stream approximations to radiative transfer in planetary atmospheres: A unified description of existing methods and a new improvement. *J. Atmos. Sci.* v. 37:630-643.

Neckel, H., D. Labs (1981). Improved data of solar spectral irradiance from 0.33 to 1.25μ. *Solar Physics* v. 74(1), 231–249. doi:10.1007/bf00151293

Paltridge, G.W., C.M.R. Platt (1976). *Radiative processes in Meteorology and Climatology*. Elsevier Sci. Pub. Co.

Pincus, R., K.F. Evans (2009). Computational cost and accuracy in calculating three-dimensional radiative transfer: Results for new implementations of Monte Carlo and SHDOM. J. Atmos. Sci. v. 66(10), 3131-3146.

Reeves, R.G., A. Anson, D. Landen, eds. (1975). Manual of Remote Sensing American Society of Photogrammetry,1st ed. Falls Church, Va.

Ricchiazzi, P. et al. (1998). SBDART: A research and teaching software tool for plane-parallel radiative transfer in the Earth's atmosphere. *Bull. Amer. Meteor. Soc.* v. 79: 2101-2114.

Schmit, T.J. , P. Griffith, M.M. Gunshor, J.M. Daniels, S.J. Goodman, W.J. Lebair (2017). · A Closer Look at the ABI on the GOES-R Series. BAMS 98(4), 681–698. (https://doi.org/10.1175/BAMS-D-15-00230.1)

Shettle, E.P.; J.A. Weinman (1970). The transfer of solar irradiance through inhomogeneous turbid atmospheres evaluated by Eddington's approximation. *J. Atmos. Sci.* v. 27, 1048-1055.

Souza, J.D., B.B. Silva, J.C. Ceballos (2008). Estimativa de radiação solar global à superfície usando um modelo estocástico: Caso sem nuvens (Estimate of global solar radiation at ground level using a stochastic model: Cloudless case). *Rev. Brasil. de Geofísica*, v. 26(1):31-44.

Thekaekara, M. (1973). Solar energy outside the Earth's atmosphere. *Solar Energy,* 14(2), 109–127. doi:10.1016/0038-092x(73)90028-5

Wallace, J.M., P.V. Hobbs (2006). *Atmospheric Science. An introductory survey*. Academic Press, 2nd. Ed, 483 pp.

Wen, G., A. Marshak, R.F. Cahalan (2008). Importance of molecular Rayleigh scattering in the enhancement of clear sky reflectance in the vicinity of boundary layer cumulus clouds. J. Geophys. Res. v.113, D24207, doi:10.1029/2008JD010592.

Zdunkowski, W., Th. Trautmann, A. Bott (2007). *Radiation in the Atmosphere. A Course in Theoretical Meteorology*. Cambridge Univ. Press, 482 pp.